Tectonics®

RESEARCH ARTICLE
10.1029/2023TC008195

Key Points:

- Kinematic model for the Santa Bárbara System shows a 1st-order detachment at 23 km depth, contributing to 18.4 km of Cenozoic shortening
- Deformation shows spatiotemporal variations, linked to reactivation of Cretaceous extensional faults and/or basement heterogeneities
- Seismicity is closely associated with deep faults rather than shallow structures affecting the sedimentary cover

Supporting Information:

Supporting Information may be found in the online version of this article.

Correspondence to:

A. Arnous,
aarnous@mendoza-conicet.gob.ar;
aarnous.aa@gmail.com

Citation:

Arnous, A., García, V. H., Pingel, H., Giambiagi, L., & Strecker, M. R. (2024). Kinematic evolution of the Santa Bárbara System in the foreland of the Central Andes of northwestern Argentina (26°S). *Tectonics*, *43*, e2023TC008195. https://doi.org/10.1029/2023TC008195

Received 22 NOV 2023
Accepted 25 MAY 2024

Kinematic Evolution of the Santa Bárbara System in the Foreland of the Central Andes of Northwestern Argentina (26°S)

Ahmad Arnous[1,2], Victor H. García[3], Heiko Pingel[2], Laura Giambiagi[1], and Manfred R. Strecker[2]

[1]IANIGLA-CONICET, Mendoza, Argentina, [2]Institut für Geowissenschaften, Universität Potsdam, Potsdam, Germany, [3]Grupo de Investigación en Geología Sedimentaria, Especialidad de Ingeniería Geológica, Departamento de Ingeniería, Pontificia Universidad Católica del Perú, San Miguel, Perú

Abstract Compared to the thin-skinned Subandean foreland fold-and-thrust belt of northern Argentina and Bolivia, the tectonically active morphotectonic province of the Santa Bárbara System in the Andean broken foreland of northwestern Argentina is characterized by a temporally and spatially disparate deformation style. Although there is no well-defined orogenic deformation front associated with the uplift of these basement-cored, reverse-fault bounded mountain ranges, there has been an overall eastward trend in Andean compressional deformation since the Miocene. While reactivation of basement anisotropies, such as early Paleozoic metamorphic fabrics and Cretaceous normal faults, has been proposed to have profoundly affected deformation processes in the Santa Bárbara System, other mechanisms involving Mesozoic and Cenozoic cover rocks may also have played an important role in orogenic deformation in this sector of the Andean foreland. We present structural field observations, interpretations of seismic reflection profiles, and kinematic modeling from the basins bordering the Candelaria Range in the southern sector of the Santa Bárbara System at 26°S. Our analysis features a 110-km-long structural cross section that images and links deep-seated structures with shallow neotectonic faults. We find that regional shortening has been facilitated by several faults associated with a regional detachment at a depth of 23 km, resulting in total horizontal shortening of about 17% (18.4 km). While the deep-seated first-order structures seem closely linked to seismogenic processes in the Andean foreland, shallow second-order structures within the sedimentary cover modify the intermontane landscapes and appear to be associated with aseismic creep.

1. Introduction

Foreland basins constitute valuable sedimentary geological archives that help explain the complex relationships between tectonic processes and the build-up of topography within mountain belts as well as the role of climate-driven variations in the surface-process regime (e.g., DeCelles, 2012). They also play a crucial role in deciphering the formation of georesources, the characteristics of regional fluid flow, the compressional reactivation of crustal zones of weakness far from plate boundaries (DeCelles, 2012; Giambiagi et al., 2022; Hilley et al., 2005; Kley & Voigt, 2008; Madritsch et al., 2008; Marshak et al., 2000; Oliver, 1986; Pfiffner, 2017), and spatially disparate seismic hazards (Costa et al., 1999, 2018). Moreover, at the scale of mountain building at convergent margins, the tectono-sedimentary evolution of forelands can provide important insights into the subduction regime and regional plate-tectonic boundary conditions, particularly with respect to plate interaction and the angle of the subduction zone (e.g., DeCelles, 2012; Horton et al., 2022; Jordan et al., 1983; Pons et al., 2023; Ramos et al., 2002; Rodriguez Piceda et al., 2023).

In the foreland of the Central Andes, two end-member styles of deformation exist in close spatial proximity to each other, involving either thin- or thick-skinned deformation and accommodating eastward shortening and orogenic growth (reviewed in Strecker et al. (2012)): (a) a wedge-shaped, thin-skinned fold-and-thrust belt with gently dipping décollements in the Subandean belt of Bolivia and northwestern Argentina (e.g., Dunn et al., 1995; Echavarria et al., 2003; McQuarrie et al., 2005); and (b) thick-skinned structures with localized uplifts bounded by high-angle reverse faults that often involve the reactivation of crustal-scale heterogeneities (e.g., Jordan et al., 1983). The latter characterize the Sierras Pampeanas of central-western Argentina and the Santa Bárbara System of northwestern Argentina (Figure 1) (e.g., Cristallini et al., 2004; Jordan et al., 1983; Kley & Monaldi, 2002). In contrast to the thin-skinned Andean fold-and-thrust belts, which feature a well-developed orogenic

10.1029/2023TC008195

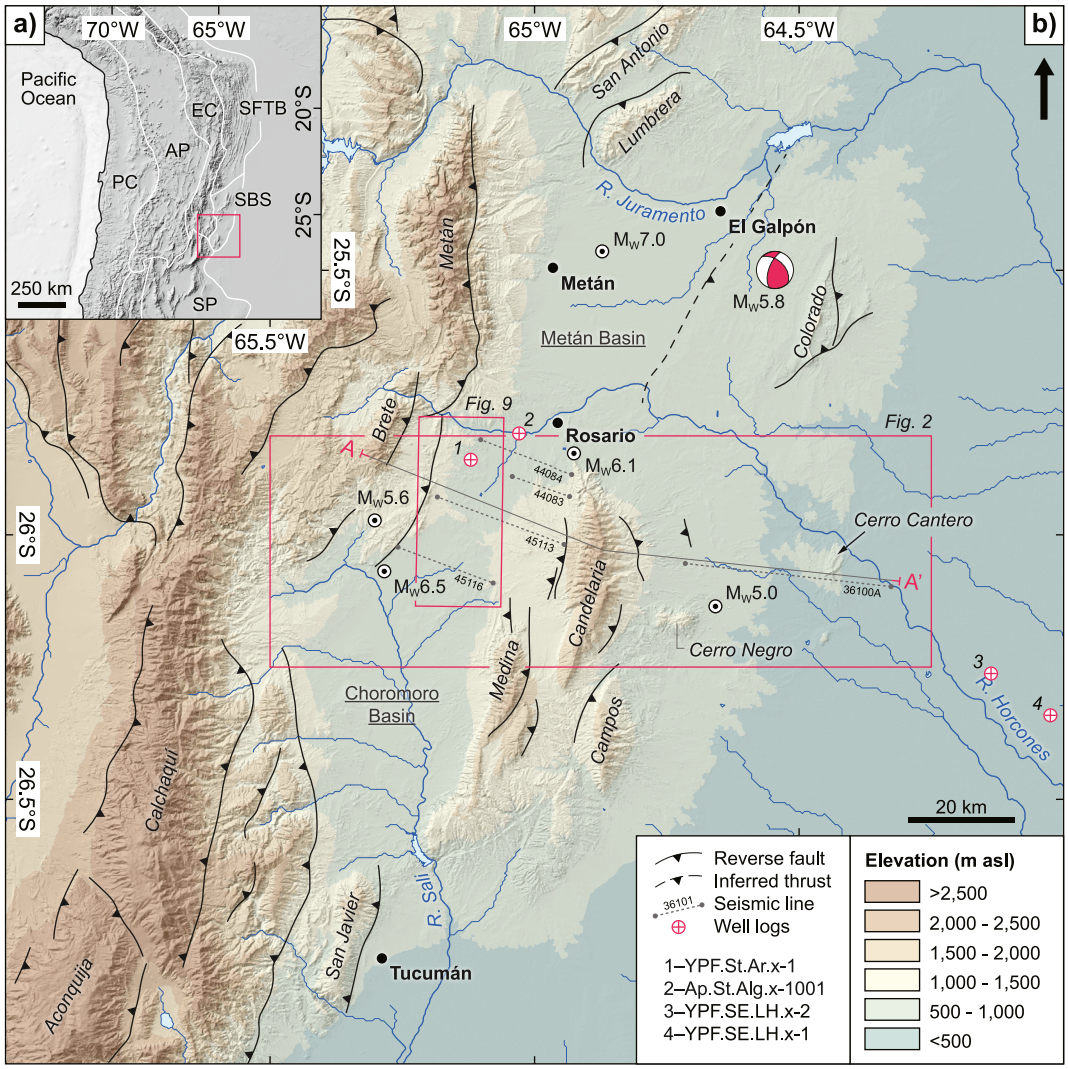

Figure 1. (a) Shaded relief map showing the location of study area (red box) in the context of Andean morphotectonic provinces (white lines). PC: Chilean Precordillera, AP: Altiplano-Puna Plateau, EC: Eastern Cordillera, SFTB: Subandean fold-and-thrust belt, SBS: Santa Bárbara System, SP: Sierras Pampeanas. (b) Topography of the Santa Bárbara System and adjacent provinces showing major reverse faults, seismic lines, epicenters of selected major earthquakes in the upper crust (INPRES, 2022), and the location of the reconstructed structural section (A–A′) presented in Figure 7.

front and a pronounced along-strike extent of high-frequency, low-amplitude folds, the thick-skinned broken foreland sectors exhibit spatially isolated range uplifts and lack an active deformation front marking the boundary between the orogen and the undeformed foreland (Figure 1; e.g., Allmendinger et al., 1983; Jordan et al., 1983).

Since early attempts to classify different foreland deformation styles in the context of geodynamic forcing mechanisms, numerous structural studies of broken forelands have revealed a high degree of structural complexity involving hybrid thick- and thin-skinned deformation within the same area (reviewed in Lacombe and Bellahsen (2016)). The two styles of deformation are thus not mutually exclusive and may evolve either synchronously or diachronously, yet the particular structural characteristics and systematics of this type of deformation in most broken-foreland areas remain enigmatic.

The most prominent unifying characteristics of active broken-foreland provinces are the wide distribution of seismicity and evidence of neotectonic deformation, often associated with reactivated basement anisotropies inherited from earlier extensional and/or contractional deformation (e.g., Figueroa et al., 2021; Grier et al., 1991; Jordan & Allmendinger, 1986; Mon & Salfity, 1995; Ramos et al., 2002). Compared to extensive fault arrays, which may trigger strong earthquakes along the frontal structures of thin-skinned fold-and-thrust belts (e.g.,

Brooks et al., 2011; Mugnier et al., 2013), reactivated pre-existing faults with shorter segments in broken forelands are generally characterized by low to medium earthquake magnitudes (e.g., García et al., 2013, 2019). However, during the post-seismic relaxation phase, such events can redistribute, modifying the state of stress of inactive, neighboring faults and triggering clusters of large earthquakes with pronounced deformation phenomena (Arrowsmith et al., 2017).

In light of these differences, deciphering the deformation history on a variety of timescales from hundreds and thousands of years to long, geological timescales constitutes an important challenge, especially with respect to an evaluation of seismic hazards. This is due to the combination of the complex geologic framework of such regions and the long periods of seismic quiescence separating single or temporally clustered earthquakes (e.g., Alvarado & Ramos, 2011; Costa et al., 2018; Landgraf et al., 2017; Patyniak et al., 2017). With respect to the longer, geological timescales, three fundamental aspects emerge that need to be addressed for a better understanding of the tectonic activity of broken forelands, which is the objective of this study: (a) the manner in which deformation propagates in space and time; (b) the role of inherited crustal heterogeneities as potential nucleation zones for spatially and temporally disparate reverse faulting; and (c) the relationships between basement structures, tectonic transport, and localized thin-skinned deformation. Understanding these aspects is also crucial for assessing the seismic hazards of broken forelands and determining measures to mitigate vulnerability.

In this study, we examine the structural evolution of the central sector of the Santa Bárbara System in northwestern Argentina. This area is covered by a network of commercial seismic reflection profiles and borehole information that allow a critical evaluation of the different deformation styles associated with deep-seated structures. Our focus is on an east-west oriented regional swath profile through the Santa Bárbara System that encompasses the basement uplift of the Candelaria Range and the adjacent Choromoro and Metán intermontane basins (Figure 1). Previous studies in this region suggest that these spatially isolated compressional basins and ranges document the transition from a formerly contiguous foreland basin to a broken foreland, which is closely linked with the reactivation of pre-existing extensional structures of the Cretaceous Salta rift basin (e.g., Cristallini et al., 1997; Kley & Monaldi, 2002; Mon & Salfity, 1995). We are specifically concerned with three types of Cenozoic faults that drive deformation in this part of the broken foreland: (a) inverted Cretaceous normal faults; (b) flexural-slip faults related to thin-skinned deformation in the sedimentary cover units; but we additionally consider (c) thrusts that nucleated in Paleozoic foliation fabrics inherited from previous orogenic processes (Mon & Hongn, 1991). In addition to previous findings, we use observations from surface geology, seismic reflection and well data, results from our own near-surface geophysical surveys (Arnous et al., 2020), and 2-D kinematic forward modeling to constrain the structural style of this region and shed light on the factors controlling its tectonic evolution.

2. Geological Setting

The Santa Bárbara System is located between 23° and 27°S. It is bounded by the Subandean fold-and-thrust belt to the north, the reverse-fault bounded Sierras Pampeanas to the south, and the thick-skinned Eastern Cordillera and the orogenic Altiplano-Puna Plateau to the west (Figure 1a; Allmendinger et al., 1983). The Santa Bárbara System comprises several isolated reverse-fault bounded and basement-cored mountain ranges as well as intermontane basins with variable degrees of neotectonic deformation and fluvial connectivity (Figure 1b; Arnous et al., 2020; Barcelona et al., 2014; Iaffa et al., 2013; Kley & Monaldi, 2002; Strecker et al., 2012). Together with the Medina, Nogalito, and Campos ranges, the basement-cored Candelaria Anticline (i.e., Candelaria Range, 2,400 m a.s.l.) is part of an elevated region surrounded by extensive sedimentary basins; these low-elevation sectors at an approximate elevation of 900 m comprise the Choromoro Basin to the west, the Metán Basin to the north, the Tucumán Basin to the south, and the largely undeformed, low-relief Chaco-Paraná foreland to the east (Figures 1 and 2). Other topographic features relevant to this study are the Metán (2,800 m a.s.l.) and Brete (2,400 m a.s.l.) ranges situated along the western transition to the Eastern Cordillera (Figure 1).

The regional basement comprises strongly deformed upper Neoproterozoic to lower Cambrian phyllites of the Puncoviscana and Medina formations, exposed mainly at the core of the Candelaria Range (Figure 2; Bossi, 1969; Turner, 1960). Along the western flank of the Candelaria Range, these rocks are unconformably overlain by discontinuous shallow-marine quartzites of the Cambro-Ordovician Candelaria Formation (Ricci & Villanueva, 1969) (Figure 3). Furthermore, Devonian shallow-marine to continental deposits of the Rincón Formation (Padula et al., 1967) crop out at Cerro Negro and in the core of Cerro Cantero (Figure 2) and have been

10.1029/2023TC008195

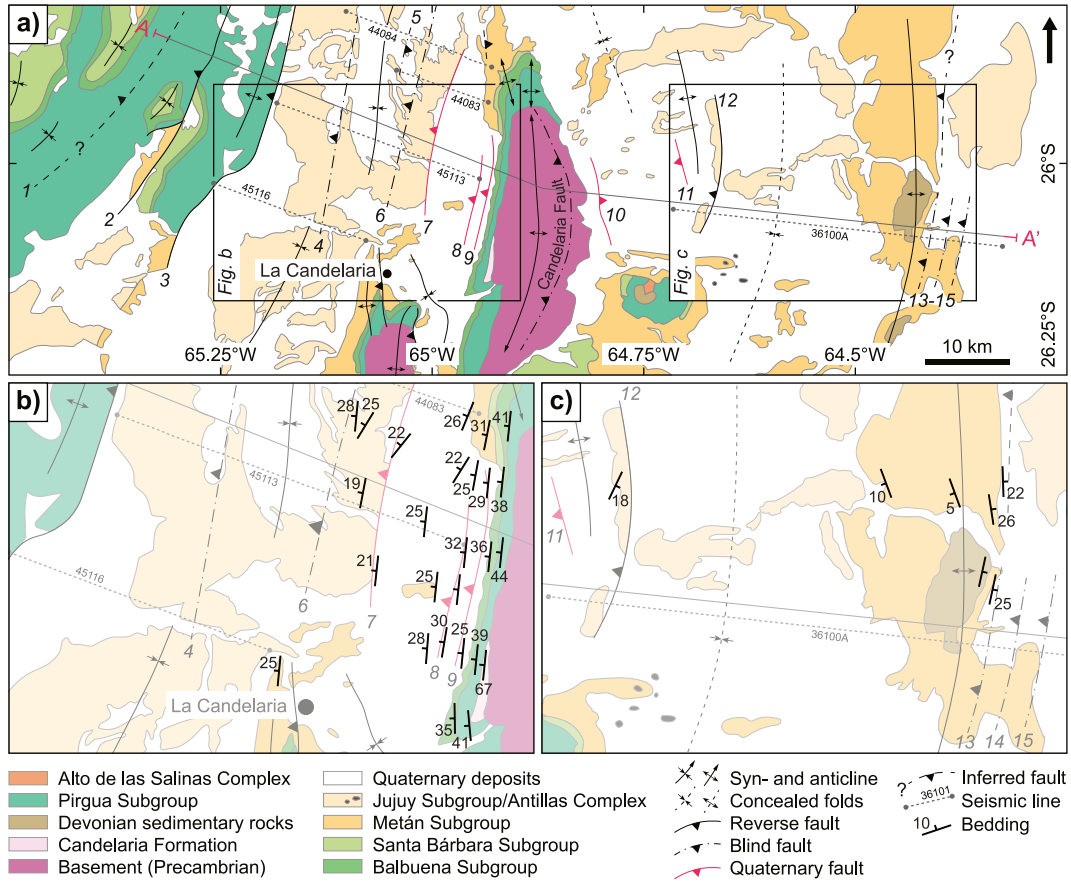

Figure 2. (a) Geological map of the Candelaria Range showing locations of mapped faults and seismic lines (modified after; Barcelona et al., 2014; Iaffa et al., 2011; Invernizzi et al., 2014; Maffucci et al., 2015; Salfity & Monaldi, 2006). (b and c) Zoom-in maps from west and east of the Candelaria Range showing structural measurements (this study). Line A-A′ denotes the location of the cross section shown in Figure 7. Labeled faults are: 1–Las Animas; 2–Iglesia; 3–El Brete; 4–El Arenal; 5–El Algarrobal; 6–Los Sauces; 7–San Esteban; 8–Barba Yaco; 9–Arias; 10–El Quemado; 11–Copo Quile; 12–San Pedro; 13–Eastern Cantero; 14–Central Cantero; and 15–Western Cantero faults.

encountered in petroleum exploration wells in the Chaco Plain to the east (Figure 3; Iaffa et al., 2011; Mon & Gutiérrez, 2007). Separated by a major unconformity, Cretaceous-Paleogene syn- and post-rift strata of the Salta Group overlie these units, which consist of syn-rift alluvial strata and fluvial redbeds of the Pirgua Subgroup overlain by continental clastic sediments and shallow marine to lacustrine limestones of the post-rift Balbuena and Santa Bárbara subgroups (e.g., Salfity & Marquillas, 1994; Figures 2 and 3). Finally, syn-orogenic Cenozoic sediments of the Andean foreland, represented by continental strata of the Mio–Pleistocene Orán Group, unconformably overlie the Salta Group and older units (Gebhard et al., 1974; Hain et al., 2011; Reynolds et al., 1994, 2000; Russo & Serraiotto, 1978). The Oran Group has been subdivided into the Metán (ca. 15–10 Ma) and Jujuy (ca. 10–1 Ma) subgroups, which are well exposed in the Andean broken foreland (Figure 2) and contain several unconformities that reflect their syntectonic character (e.g., Cristallini et al., 1997; Hain et al., 2011; Iaffa et al., 2011).

3. Methods

We analyzed five seismic reflection lines (obtained from Secretaría de Minería y Energía de Salta), four in the northern sector of the Choromoro Basin (lines 44084, 44083, 45113, and 45116) and one east of the Candelaria Range (line 36100A). All seismic lines provided records that surpassed 4.8 s two-way travel time, and the basement was typically imaged within 3.3 s. The Choromoro lines are between 18 and 23 km long and about 2.5 km apart. Furthermore, we obtained four industry reports (Figure 4) that record the stratigraphy of wells

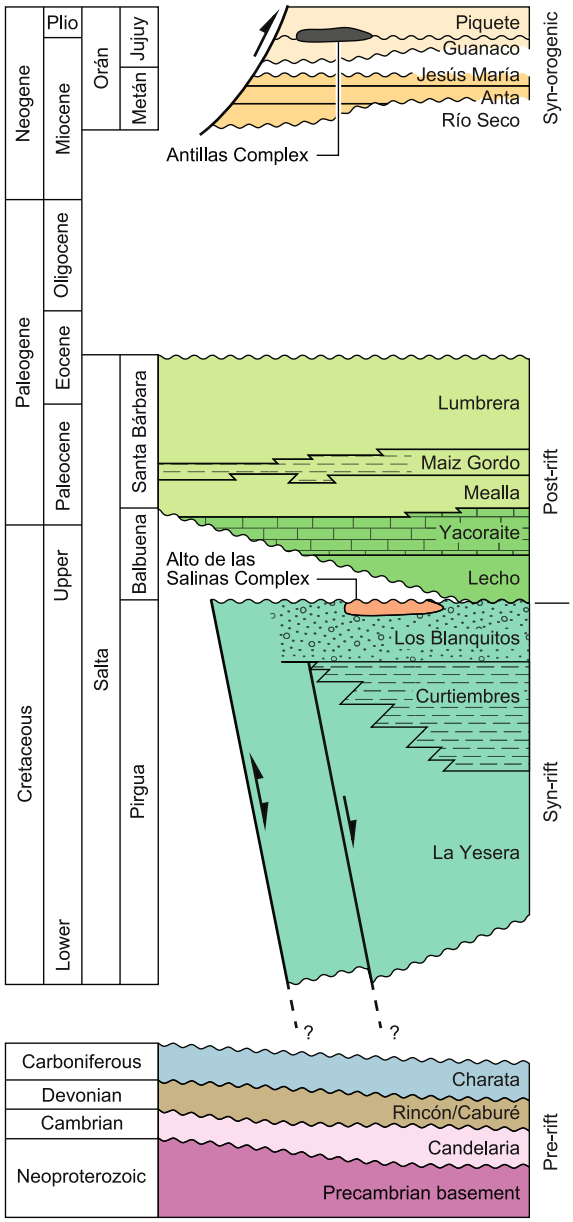

Figure 3. Stratigraphy of the study area (modified after Carrera et al., 2006; Invernizzi et al., 2014; Maffucci et al., 2015; Marquillas et al., 2005).

located to the northwest of the Candelaria Range (YPF.St.Ar.x-1 operated by YPF in 1973 and Ap.St.Alg.x-1001 operated by Shell Capsa in 1989) and the Los Horcones wells (LH x-1 and LH x-2), located in the Chaco Plain both operated by YPF between 1971 and 1973. The well reports contain a description of the lithology and the depth of tops of the principal stratigraphic units that were used to tie the wells to the seismic profiles. Based on the stratigraphic characteristics identified in the well reports and the corresponding changes in reflectors, we identified different seismic stratigraphic packages and grouped them into four principal sequences; from bottom to top (sequences 1–4) these are represented by the syn-rift, post-rift, and two syn-orogenic foreland sequences. Depth conversion of the seismic reflection data was performed using interval velocities calculated from a velocity table derived from the well data and seismic-line preprocessing data (for details see Text S1 and Table S1 in Supporting Information S1).

In addition, structural field data was incorporated in a new geological-structural map, from which the thicknesses of the sedimentary sequences were estimated. Combined information from well logs and mapped lithological contacts at the surface aided in the interpretation of the seismic profiles. Nevertheless, due to significant noise in the seismic lines (Figure 5), particularly evident in seismic line 36101 in Figure 5e, the interpretation was primarily based on kinematic forward modeling. Each fault was analyzed using a trial-and-error procedure involving various geometries to replicate the folding pattern seen in the easternmost region, to generate uplift, and to achieve the optimal manner to reproduce the geometries observed in outcrops. To simulate fault evolution and associated folding of the sedimentary cover rocks we also applied the Trishear deformation method proposed by Erslev (1991) and the principles of fault-bend folding outlined in Medwedeff (1989). The identified faults were modeled using the MOVE software (version 2017) structural geology software (Petroleum Experts) to account for variations in inclination and ramp geometry, providing input for the subsequent construction of the structural cross-section model within the same software package. The 110-km-long regional cross-section, approximately perpendicular to the main structures of the study area, was constructed by integrating the geological-structural map, the estimated sequence thicknesses, well data, and the interpretation of the seismic profiles, using MOVE. The cross section encompasses the region with the highest density of available field data and captures the most representative structures (section A-A′, Figure 2). The model was divided into two scales: (a) a large scale, focusing on deep-seated detachment faults, and (b) a smaller scale, targeting neotectonic near-surface structures (for details see Texts S2, S3, and Table S2 in Supporting Information S1).

4. Results

4.1. Well-Log Stratigraphy

Two wells located to the northwest of the Candelaria Range (YPF.St.Ar.x-1 and Ap.St.Alg.x-1001) have similar penetration depths to ca. 3.5 km below the surface and good coverage of sedimentary sequences in the foreland, including the Jujuy (0.8–1.3 km), Metán (1.3–1.5 km), Santa Bárbara (0.4–0.8 km), and Balbuena (0.3–0.4 km) subgroups (Figure 4). Moreover, Ap.St.Alg.x-1001 reached the Pirgua Subgroup (syn-rift), penetrating it for about 600 m. In contrast, the Los Horcones wells (LH x-1 and LH x-2), located in the Chaco Plain, reveal a significantly thinner syn-orogenic sequence that directly overlies Paleozoic sedimentary rocks, and contains no record of the Salta Group (Figure 4).

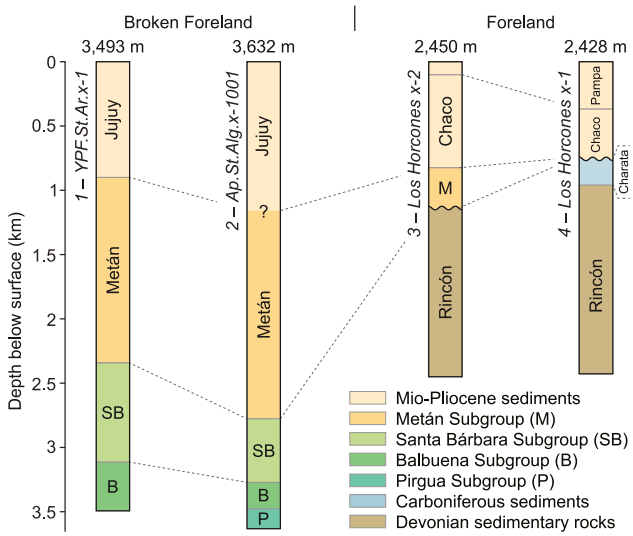

Figure 4. Stratigraphic profiles interpreted from exploration wells. For locations see Figure 1b.

4.2. Interpretation of Seismic Reflection Lines

Seismic reflection lines from the Choromoro Basin image well-defined, continuous reflectors of the uppermost sedimentary units, followed by short and discontinuous high acoustic impedance reflectors corresponding to the seismic basement (Figures 5a–5e). Using the borehole data, we correlated the main lithological units with the seismic sequences. The upper part of the imaged foreland sequence was assigned to the Jujuy Subgroup, which is characterized by poor to medium reflectivity with low frequency and poor lateral continuity. This sequence records intraformational growth-strata patterns (i.e., onlapping strata in Figures 5c and 5e). Below these units appear the reflectors of the Metán Subgroup, which are characterized by high frequency and good lateral continuity, in addition to well-developed reflectivity. Separated by a gentle unconformity, this Miocene sedimentary package covers the post-rift sequence, whose reflectors can be identified by very strong reflectivity and pronounced continuity; this specifically applies to the Balbuena Subgroup, which is a regional marker horizon well suited for seismic interpretation and structural reconstructions (e.g., Kley et al., 2005). The final group of reflectors is characterized by strong and continuous reflectivity. These strata can be assigned to the syn-rift Pirgua Subgroup, which lies unconformably on seismic basement. In addition, we identified three new faults, namely the El Algarrobal (5), Los Sauces (6), and San Esteban (7) faults, and confirmed the location of the El Arenal Fault (4) discussed in Seggiaro et al. (2015). In the eastern part of lines 44084, 44083, 45113 (Figures 5a–5c), reflectors dip ∼30–35° to the west, representing the western back limb of the basement-cored Candelaria range. Here, noisy reflectors at depths between 1,000 and 3,000 m indicate the presence of metamorphic basement. Above the basement, a low-angle unconformity is observed, which is characterized by strong reflections and high acoustic impedance, typical of the Pirgua Subgroup (Iaffa et al., 2011) (Figure 5).

4.2.1. El Arenal Anticline

Lines 44084, 45113, and 45116 (Figure 5), in the Choromoro basin provide a clear image of the El Arenal Fold (Seggiaro et al., 2015). It is an asymmetrical, east-verging anticline with a wavelength of 5 km. Importantly, this structure affected the entire sedimentary sequence, including the strata of the Jujuy Subgroup, although to varying degrees. While lines 44084 and 45113 exhibit marked onlapping in the Jujuy Subgroup, indicating the syn-depositional growth of the El Arenal Anticline, no such growth strata are observed on line 45116 (Figure 5d) in the southern sector of the structure. Based on our interpretation and kinematic analysis, we infer that this structure is related to the El Arenal Fault (4), an east-verging blind thrust, which emerges at ca. 20–30° from a shallow detachment level at ca. 4 km depth.

As seen in lines 45113 and 45116, the fault propagated along a 19°W-dipping ramp with a slip of ca. 5 km, while line 44084 shows a ramp angle of 30°W and slip of about 3.5 km, resulting in 2.4 and 1.5 km of horizontal shortening, respectively.

4.2.2. Los Sauces Anticline and San Esteban Fault

In the central part of line 44084 (Figure 5a), a symmetrical anticline is imaged, that is interpreted to be related to motion along two high-angle reverse faults rooted at shallow depth within the basement. These structures are: (a) the Los Sauces Fault (6), which dips 57° to the west with a slip of approximately 500 m; and (b) the El Algarrobal Fault (5), which dips 58° to the east, with a slip of 700 m. The displacement along these faults generated a pop-up-style anticline with negligible surface expression, since it grew synchronously with the sedimentation of the Jujuy Subgroup, followed by Quaternary sediments that covered the structure (Figure 5a). The shortening associated with this structure is 260 m. On seismic line 44083 (Figure 5b), the observed displacement along the Los Sauces Fault, which dips ∼75° to the west in this section, is between 360 and 400 m. Progressive unconformities within the Jujuy Subgroup, specifically in the Guanaco and Piquete formations, indicate syntectonic sedimentation during the Mio–Pliocene. In the upper part of seismic line 45113 (Figure 5c), onlap geometries were also recognized in the strata corresponding to the Jujuy Subgroup and interpreted accordingly as growth strata.

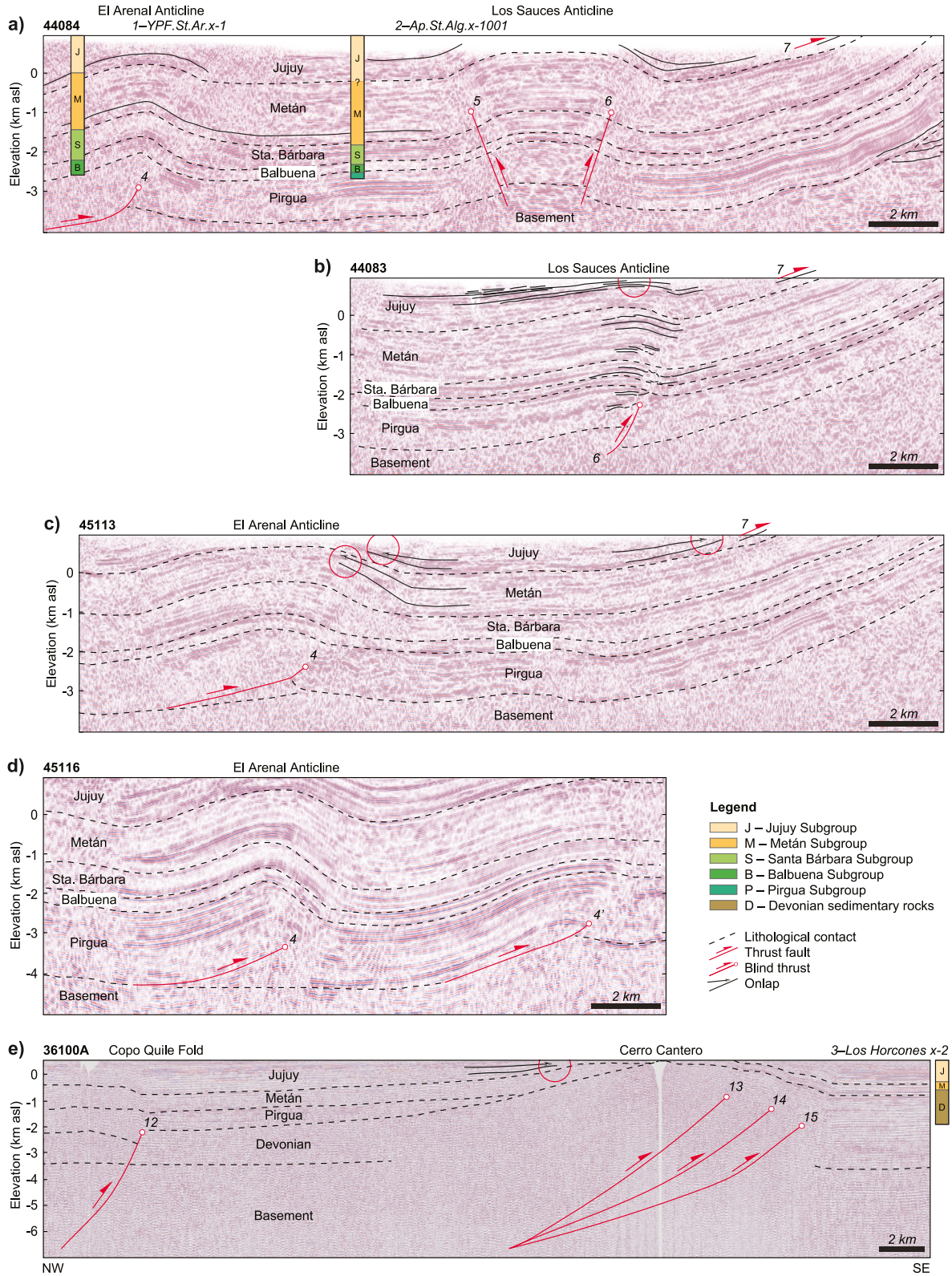

Figure 5. 2-D seismic lines with structural and stratigraphic interpretation. For location see Figures 1 and 2. Labeled faults are: 4–El Arenal; 5–El Algarrobal; 6–Los Sauces; 7–San Esteban; 12–San Pedro; 13–Eastern Cantero; 14–Central Cantero; and 15–Western Cantero faults. An uninterpreted version of the seismic lines can be found in Figure S3 of the Supporting Information S1.

The San Esteban Fault (7, Barcelona et al., 2014), uplifted conglomeratic alluvial fan deposits of the Jujuy Subgroup and is observed in lines 44084, 44083, and 45113 (Figures 5a–5c). These seismic lines reveal that the reflectors associated with this structure are mostly continuous. However, since a topographical expression of ∼40 m forms a fault scarp at the surface, we propose the existence of a bedding-parallel, flexural-slip fault within the Jujuy Subgroup.

4.2.3. Line 36100A and Deformation at Cerro Cantero

East of the Candelaria Range, seismic line 36100A (Figure 5e) runs for about 40 km in WNW-ESE direction, crossing the Cerro Cantero (Figures 1 and 2). Stratigraphic information for the seismic interpretation is provided by wells LH x-1 and LH x-2 (Figure 4), located about 40 km southeast of Cerro Cantero. As stated in Section 4.1, these wells document a significantly reduced thickness of the foreland sequence that immediately overlies Devonian sedimentary rocks, with no depositional record of the Salta Group (Figure 5)—a stratigraphic setting confirmed by surface geology at Cerro Cantero (Figure 2). The resolution of line 36100A is not high enough to unambiguously identify the contact between Devonian strata and the underlying basement rocks; therefore, our interpretation of the location of the contact in Figure 5 should be taken with caution. In the central sector of line 36100A, west of Cerro Cantero, the stratigraphy is not very clear as there is no additional subsurface information to help with the seismic interpretation. However, outcrop information from nearby Cerro Negro (Figure 2) suggests that the Pirgua Subgroup unconformably overlies the Devonian strata. Similarly, surface geology confirms the presence of the entire section of the Metán Subgroup (ca. 1,000 m), whose thickness we consider to be mostly constant in the profile and which is overlain by the Jujuy Subgroup. Since the Pirgua Subgroup is not present at Cerro Cantero and farther east, we propose an eastward lateral pinch-out of this unit.

In seismic line 36100A, we identified four main structures: a high dipping reverse fault to the west (12, Figure 5e) and three reverse faults underneath Cerro Cantero (13–15, Figure 5e). The subvertical structure in the western sector correlates with the San Pedro Fault (12) at surface, juxtaposing Devonian strata over the Pirgua Subgroup. Here, thickness variations in the Pirgua Subgroup and folded Cenozoic foreland strata suggest that this structure is a steeply dipping reverse fault. The three 30–45°W-dipping reverse faults, in the eastern sector, are associated with fault-propagation folding and uplift of the Cerro Cantero. Growth strata in the Jujuy Subgroup document syn-tectonic sedimentation on both sides of Cerro Cantero and thus a late Miocene onset for the contractional deformation associated with this structure. As the seismic line is characterized by noise interference, the interpretation of faults 13, 14, and 15 necessitated a Trishear modeling approach (Erslev, 1991) to accurately determine their position and geometry. Our objective was to replicate the three folds on the eastern side of the Cerro Cantero, ensuring consistency with the measured bedding on both flanks of the Cerro Cantero fold on the surface. The optimal approach involved positioning the fault tips at the frontal syncline and linking them at a depth of 6 km (Figure 5e).

5. Balanced Cross Section

Our balanced cross-section analysis reveals that, during the late Cenozoic, the southern Santa Bárbara System and segments of the Eastern Cordillera underwent a cumulative horizontal crustal shortening of 18.4 km over a lateral distance of 110 km, representing 16.7% of the total shortening (Figure 6). This compressional deformation was facilitated by a variety of faults, categorized into first-, second-, and third-order structures based on their estimated offsets. More details about these structures are provided below (for details see Texts S2–S4, Table S2, and Figure S2 in Supporting Information S1).

5.1. First-Order Structures

Shortening across the investigated section is primarily accommodated by partially inverted Cretaceous normal faults, namely the Las Animas (1), Iglesia (2), and El Brete (3) faults in the Eastern Cordillera to the west, as well as the San Pedro Fault (12) situated at the center of our reconstructed section (Figures 2 and 6). The geometry of the Candelaria Fault is interpreted as listric to (a) account for the asymmetric folding observed in the Mesozoic to Cenozoic sedimentary cover strata along the western and eastern flanks of the Candelaria Range (Figure 6); and (b) the gradual decrease in stratal dips observed in seismic reflection data from the Choromoro Basin (Figures 5a–5c). Furthermore, foreland-ward propagation of Cenozoic contraction has produced three parallel reverse faults on the eastern flank of Cerro Cantero, here referred to as the eastern (13), central (14), and western (15) Cerro

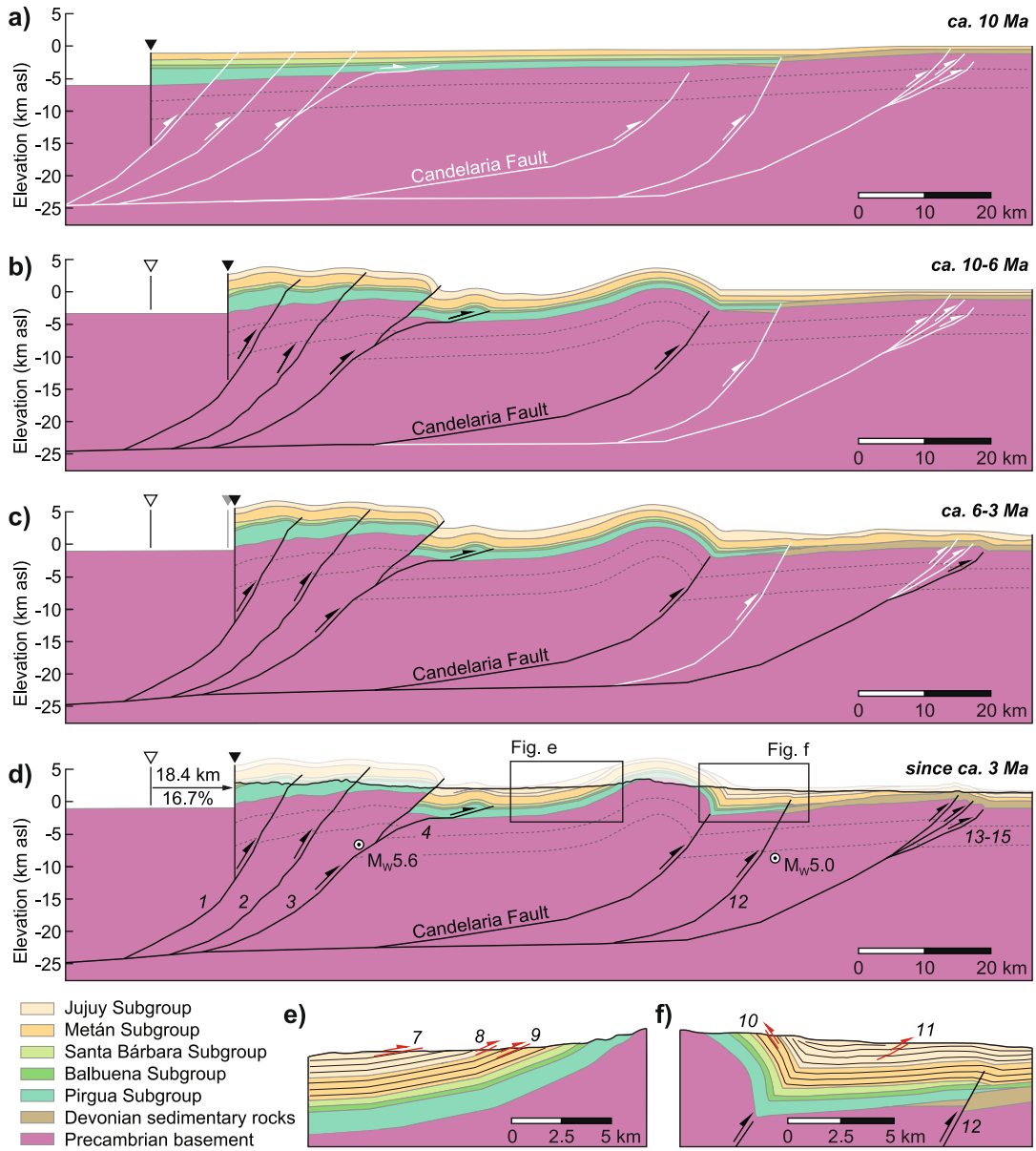

Figure 6. (a) Undeformed initial model (prior to 10 Ma), (b and c) intermediate models between 10–6 Ma and 6–3 Ma, and (d) final forward-modeled kinematic reconstruction of our structural cross section. (e and f) Detailed view of areas bordering the Candelaria Range. Circles show $M_W \geq 5$ earthquake hypocenters recorded in 2021 and 2022 (INPRES, 2021, 2022). Labeled faults are: 1–Las Animas; 2–Iglesia; 3–El Brete; and 4–El Arenal faults. Faults shown in black represent active faults in the corresponding time period.

Cantero faults (Figures 5e and 6). According to our model, we suggest that all these first-order faults originate from a basal detachment at approximately 23 km depth (Figure 6), resulting in a cumulative shortening of 16.1 km along these structures. In our model, the Las Animas (1), Iglesia (2), and El Brete (3) faults were active at approximately 10 Ma, playing a crucial role in generating uplift and loading, thereby inducing flexure in the area where the Choromoro basin currently resides (Figures 6a and 6b). Subsequently, the activity of the Candelaria Fault began around 9 Ma, with all the aforementioned faults remaining active concurrently. Later, at around 4 Ma, faults 15, 14, and 13 were generated in sequential order and have remained active since then, continuing to exert influence until the present day (Figures 6c and 6d).

5.2. Second-Order Structures

The blind El Arenal Fault (4) within the Choromoro Basin generated a second-order fault-propagation fold in the overlying sedimentary strata of the Jujuy Subgroup. According to our model, a detachment fault initiated during the middle to late Miocene (Figures 5c and 6) at the basement-Pirgua Subgroup interface at 4 km depth and then propagated eastward and upward along a fault ramp dipping between 19° and 30°W. The estimated shortening along this structure is 2.1 km. Notably, growth strata in the Jujuy Subgroup are observed on both limbs of the anticline, constraining the initiation of folding to the late Miocene. Moreover, seismic line 44084 (Figure 5a) revealed the presence of the Los Sauces (5) and El Algarrobal (6) blind reverse faults, which are inferred to be responsible for the pop-up geometry of the Los Sauces Anticline (see Section 4.2.2). Similar to the El Arenal Anticline, seismic lines 44084 and 44083 (Figures 5a and 5b) reveal intraformational onlaps within the Jujuy Subgroup in the hanging wall of the Los Sauces Fault (6), implying late Miocene–Pliocene structural growth. Shortening across this structure is estimated to be 200 m.

5.3. Third-Order Structures

Third-order faults identified in this study accommodate contractional deformation in the western and eastern piedmont regions of the Candelaria Range (Figures 6d–6f). As these faults exclusively affect the Miocene to Pleistocene sedimentary cover, including Quaternary alluvial fans (see Section 4.2.2), the study area can clearly be classified as a neotectonically active region.

More specifically, the western foothills of the Candelaria Range exhibit two bedding-parallel (dipping 30°W) flexural-slip faults (8 and 9 in Figure 6e, see also Figure S1a in Supporting Information S1) that nucleate at the base of incompetent layers within the Metán and Jujuy subgroups. These faults display 10-km-long, straight surface expressions and feature 5- to 30-m-high counter-slope scarps that developed in Quaternary alluvial-fan deposits. Although we cannot determine the exact timing of the activity of these faults, the regional distribution of various generations of alluvial-fan surfaces at different elevations in the piedmont suggests a Pleistocene age.

In the eastern piedmont of the Candelaria Range, the Copo Quile Fault (11) has generated an 8-km-long, N-S-striking scarp that offsets Quaternary alluvial-fan deposits (Figure 6f; Arnous et al., 2020). Structural modeling allowed us to interpret this fault as a west-dipping structure associated with a deep ramp dipping 22°W and a shallow ramp dipping 37°W. This change in the inclination of the ramps is consistent with the generation of the structure observed in the hanging wall of the fault (Figure 6d). The optimal modeling result reflecting the field relationships was achieved by starting the modeling with 2°W stratal dips, which can be attributed to prior activity of the San Pedro Fault (12) toward the east, suggesting that a displacement of 80–90 m would be required to produce a structure similar to the observed tilt of the alluvial fan. The El Quemado Fault (10) is related to flexural slip and is rooted in the contact between the strata of the Santa Bárbara and Metán subgroups on the eastern flank of the Candelaria Range, which dips 60°E according to the proposed kinematic model (Figure 6f). Fault slip was estimated to be 30–35 m in total (see Figures S1b and S1c in Supporting Information S1).

6. Discussion

The kinematic model presented in our study is a viable solution to explain deformation processes in the broken Andean foreland of northwestern Argentina. The model is compatible with a generally thick-skinned tectonic deformation east of the Eastern Cordillera, which additionally incorporates thin-skinned compressional features associated with flexural-slip faulting of Mio–Pliocene foreland strata in the intermontane basins between isolated basement-cored uplifts. Our analysis and prior studies (e.g., Barcelona et al., 2014; Iaffa et al., 2011) suggest that the localized uplifts in the Santa Bárbara broken foreland tend to occur along re-activated, high-angle structures. In this environment, the complex spatiotemporal patterns of earthquakes (Cahill & Isacks, 1992; Sanchez et al., 2013; Scott et al., 2014; Zeckra, 2020), widely distributed, highly diachronous Quaternary tectonic landforms (Arnous et al., 2020; Barcelona et al., 2014; Costa et al., 2020), and evidence of tectonic forcing of fluvial networks (Seagren et al., 2022) pose a major additional challenge to unraveling the spatiotemporal evolution of deformation and evaluating potential surface-rupture sites and extents during individual earthquakes. A further complication in the interpretation and assessment of seismic hazard is the seemingly long periods of quiescence between earthquakes in this environment (Costa et al., 2020; Ortiz et al., 2022; Zossi, 1979). To a certain extent, these characteristics are comparable to enigmatic intraplate earthquakes and deformation (e.g., Stein &

Mazzotti, 2007), emphasizing that instrumental records are strongly biased measures of future earthquake hazards in these structural settings. In this context, a rigorous inventory of faults and paleoseismological data is therefore necessary. Below, we discuss our fault inventory of the southern-central sector of the broken foreland of the Santa Bárbara System and evaluate it with respect to fault evolution and fault activity. This is a first fundamental step in analyzing the structural characteristics of a seismogenic province in the context of future paleoseismological work and hazard assessments.

6.1. Spatiotemporal Characteristics and Style of Deformation

Our 2-D kinematic model across the southern Santa Bárbara System exhibits a strong correlation with deformation features observed in the field and aligns well with interpretations drawn from seismic reflection data. Moreover, our model suggests that deformation in the southern Santa Bárbara System (26°S) is the result of crustal shortening transferred via a gently west-dipping detachment level that connects first-order structures such as the El Brete, Candelaria, and Cerro Cantero faults at depths ranging from 23 to 25 km. This estimate is consistent with previous seismic interpretations and structural models for the Santa Bárbara System that propose a detachment level around 20 km depth (e.g., Cristallini et al., 1997); this is supported by the depth distribution of earthquake clusters in our study area (Figures 7a and 7c; Zeckra, 2020) and thermomechanical models at 24°S that suggest a low-strength zone at the brittle-ductile transition at depths between 20 and 25 km (Giambiagi et al., 2022; Ibarra et al., 2021).

Onset of deformation and uplift of the Candelaria Range is well constrained by growth strata in the lower Jujuy Subgroup (~9 Ma) flanking this range (Figure 5); this suggests a nearly simultaneous propagation of deformation at this latitude of the El Brete Range, which we infer to have started at ~10 Ma, similar to the Metán Range (Hain et al., 2011). This appears to be a regional phenomenon, as mountain ranges in the northern Sierras Pampeanas and the southern Eastern Cordillera exhibit a similar timing of late Cenozoic uplift and deformation (Figures 6b, 7a, and 7b; Carrapa et al., 2011; Deeken et al., 2006; del Papa et al., 2021; Garcia et al., 2013; Hain et al., 2011; Löbens et al., 2013a; Mortimer et al., 2007; Payrola et al., 2020; Pearson et al., 2013; Pingel, Deeken, et al., 2023; Sobel & Strecker, 2003; Zapata et al., 2020). Subsequently, activity continued with slip along the Las Animas (1) and Las Iglesia (2) faults, followed by a major pulse of uplift associated with the El Brete Fault (3) (Figure 6b). This uplift of the El Brete Range (and the adjacent Metán Range to the north) was crucial for the exhumation of Cretaceous sedimentary rocks and the coeval flexural subsidence to the east. Subsequently, tectonic activity along the Cerro Cantero fault system to the east may have commenced during the Pliocene as documented by growth strata within the upper Jujuy Subgroup (ca. 4 ± 1 Ma; Figures 5e and 6c). The last deformation stage was focused on faults with small displacements, such as the San Pedro Fault (12). Similarly, our analysis suggests that the deformation recorded near the El Quemado (10) and Copo Quile (11) faults is the result of Quaternary reactivation that accommodates thin-skinned shortening in the near-surface sectors of the eastern side of the Candelaria Fault.

In contrast to the Subandean fold-and-thrust belt farther north, our results support the notion of a foreland deformation style without a systematically eastward-migrating, well-defined thrust front (e.g., García et al., 2019; Hain et al., 2011; Strecker et al., 2012). Instead, several spatially distributed structures were active simultaneously, with an onset of deformation at about 10–9 Ma (Figures 7a and 7b), while other structures may have started later and continued their activity into the Quaternary. For example, the latter scenario is supported by decreasing horizontal GPS-velocities from ca. 15 to 5 mm/yr across the eastern Andean flanks, between 22° and 29°S (Figure 7d), which indicate active shortening in the Eastern Cordillera and Santa Bárbara System (Figueroa et al., 2021; McFarland et al., 2017).

Despite the suggested presence of a deep-seated detachment, indicating thick-skinned tectonics in the Santa Bárbara System, the kinematics of shallow-dipping faults in this context—such as the El Arenal Fault—are better explained by movement along detachment levels located at a depth of 4 km. These shallow-dipping faults branch out from the inferred main detachment at the interface between the basement and the sedimentary cover rocks and thus represent transitional structures between pure thick- and thin-skinned deformation styles.

Although our derived amounts of shortening are slightly higher than those presented in earlier studies (Kley et al., 1999), the degree of shortening in the Santa Bárbara morphotectonic is significantly lower compared to the thin-skinned Subandean region (Baby et al., 1997; Echavarría et al., 2003; McQuarrie et al., 2005) and thus supports these previous analyses. There, Cenozoic Andean compression has been accommodated by the formation of décollement levels located in mechanically weak strata in a deep Paleozoic sedimentary basin; these

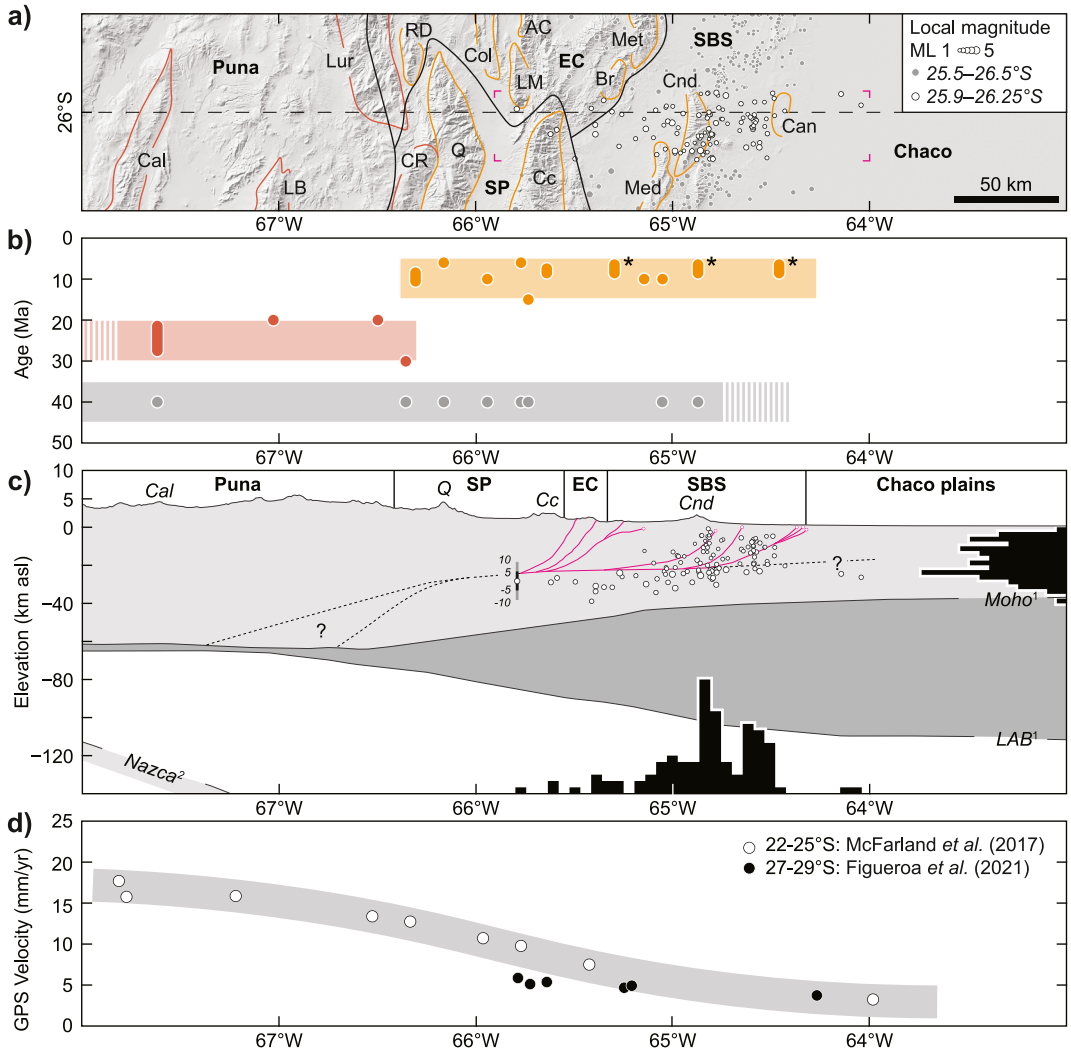

Figure 7. (a) Shaded relief map showing major mountain ranges across the northwest Argentine Andes and local seismicity (Zeckra, 2020; Zeckra & Krüger, 2023; Table S4 in Supporting Information S1) between 25.5 and 26.5°S (gray and white circles). White circles represent a subset of the seismicity data from the vicinity of the structural profile (25.9–26.25°S). Ranges: Cal–Calalaste; LB–Laguna Blanca; Lur–Luracatao; RD–Runno/Durazno; CR–Chango Real; Q–Quilmes; Col–Colorados; AC–Aguas de Castilla; LM–Leon Muerto; CC–Calchaquí; Br–El Brete; Met–Metán; Med–Medina; Cnd–Candelaria; Can–Cerro Cantero. (b) Spatio-temporal distribution of Cenozoic deformation onset estimates (gray: Eocene; red: 30–20 Ma; orange: 15–5 Ma, Pingel, Deeken, et al., 2023). The asterisk indicates estimates from this study. For more information see Table S1 in Supporting Information S1. (c) Regional cross section at 26°S showing our structural interpretation (red colored structures) of the southern Santa Bárbara System (from Figure 6) and crustal earthquake hypocenter locations between 25.9 and 26.25°S (see panel a). Note that the black and gray bars show the potential depth uncertainties (in km) of the entire seismic record: 5 and 10 km, respectively (Zeckra, 2020). The histograms on the bottom and right side of the diagram show the longitudinal and depth distribution of the earthquake hypocenters. [1]Moho and lithosphere-asthenosphere boundary (LAB) are from Ibarra et al. (2019); [2]Top of the Nazca Plate is from Hayes et al. (2018). (d) GPS-derived horizontal (eastward) surface velocities for the southern Central Andes (Figueroa et al., 2021; McFarland et al., 2017; Table S5 in Supporting Information S1).

deposits pinch out southward within the transition to the Santa Bárbara System (Allmendinger et al., 1983; Pearson et al., 2013).

On a broader regional scale involving the Andean interior, it is noteworthy that the late Cenozoic (ca. 15–10 Ma) onset of deformation and range uplift in the northern Sierras Pampeanas, the southern Eastern Cordillera, and the Santa Bárbara System (Figures 7a and 7b) discussed above coincides with an estimated surface uplift of up to 2 km in the central Puna Plateau (24°–25°S), as determined by stable-isotope paleoaltimetry (Pingel, Alonso, et al., 2023). Regardless of the possible mechanisms of such uplift, this implies a potential connection between the creation of high topography during plateau uplift and the tectonic fragmentation and isolated uplifts of the adjacent foreland (e.g., the northern Sierras Pampeanas, the southern Eastern Cordillera, and the present-day

Santa Bárbara System) through the eastward transmission of compressive stresses and, as proposed in this study, faulting along deep-seated detachment faults.

6.2. Reactivation of Inherited Zones of Crustal Weakness

According to previous studies and our observations, deformation in the Santa Bárbara System is closely related to the contractional inversion of the Cretaceous extensional faults (e.g., Grier et al., 1991; Kley & Monaldi, 2002; Iaffa et al., 2013; Pearson et al., 2013). In contrast, the potential influence of older basement heterogeneities that may have initially guided extensional deformation during Cretaceous rifting (e.g., Hongn & Riller, 2007; Hongn et al., 2010) and subsequent Cenozoic contractional reactivation remains poorly understood due to the lack of direct and validated evidence for inversion. For example, the geometries of the El Algarrobal (5) and Los Sauces (6) faults provide no conclusive evidence that Cretaceous normal faulting and later contractional reactivation occurred; this would certainly have been reflected by variations in the thickness of the syn-rift sediments of the Pirgua Subgroup. In addition, the existence of the Candelaria Fault is difficult to reconcile with contractional reactivation of inherited extensional structures, because no extension-related thickness variations of the Pirgua Subgroup can be discerned. This suggests either that Cenozoic faulting was independent of pre-existing structures or that faulting was facilitated by basement heterogeneities inherited from Paleozoic orogenic processes that affected this region, but that were not imaged in the available seismic reflection data (Hongn et al., 2010; Iaffa et al., 2011). In this context, for example, a direct link between Paleozoic basement heterogeneities, such as foliations and steeply dipping shear zones, and their reactivation in the Eastern Cordillera and the Santa Bárbara System has been proposed (e.g., Hongn & Riller, 2007; Hongn et al., 2010). While the exact nature of fault nucleation and rupture for these structures cannot be further clarified with the available data, there is a viable possibility that, as in other broken-foreland settings (e.g., Marshak et al., 2000) or regions with pronounced inherited crustal structures (Mora et al., 2006; Teixell et al., 2003). According to new modeling studies the disparate nature of faulting in the foreland might even have been facilitated by more extensive, lithospheric-scale zones of weakness in the South American continental plate as proposed by Ibarra et al. (2021) and Liu et al. (2022).

The San Pedro Fault (12) on seismic line 36100A lacks clarity concerning variations in the thickness of the Pirgua Subgroup (Figure 5e). However, although the Pirgua Subgroup is evident at Cerro Negro (Figures 1 and 2), there is no indication of its deposition east of the fault, as discussed in Section 4.2.3. This observation supports the notion that this fault is a reactivated Cretaceous normal fault.

6.3. Seismogenic Potential of Faults in the Santa Bárbara System

In general, our perception and knowledge of the location and magnitudes of earthquakes, the extent of co-seismic ruptures, and even the recurrence of earthquakes has been largely influenced by large-magnitude events that have occurred along plate boundaries (Scholz, 2002). Although there is increasing evidence of ground-rupturing earthquakes in continental interiors and regions with low deformation rates that are far from plate boundaries indicating that, these regions are indeed subject to considerable seismic hazard (England & Jackson, 2011; Stein, 2010), they are rarely highlighted on seismic hazard maps. Not only do these earthquakes in the broken foreland of the Andes recur less frequently than those originating along plate boundaries, their locations and surface ruptures are also far less predictable, and therefore pose a largely undescribed, poorly understood and unmonitored hazard (Costa et al., 2018, 2020).

The character of foreland deformation and seismicity in the Santa Bárbara System differs substantially from the seismogenic regime of the Subandean fold-and-thrust belt of northernmost Argentina and Bolivia (e.g., Figueroa et al., 2021). Although no seismogenic surface ruptures have been instrumentally recorded there, recent geodetic measurements suggest that strain accumulates along a partially locked sector of a gently dipping master basal décollement, where slip occurs continuously at down-dip positions (Weiss et al., 2015, 2016). At up-dip positions, however, the décollement remains locked until the accumulating slip is released in a rupture event (most likely an earthquake) that propagates toward the tip of the Andean orogenic wedge, which coincides with in-sequence deformation and a well-defined deformation front (e.g., Weiss et al., 2015, 2016). Given that earthquake magnitude is proportional to fault rupture area (e.g., Wells & Coppersmith, 1994), fold-and-thrust belts with wider locked zones have a greater potential for large earthquakes, leading Brooks et al. (2011) to suggest that the

easternmost, approximately 400-km-long Subandean fault scarps may be the site of megathrust earthquakes, similar to conditions inferred for the Himalayan front (e.g., Mugnier et al., 2013).

In contrast, thick-skinned broken forelands, such as the Santa Bárbara System in Argentina, form where retroarc convergence is accommodated along high-angle faults that are often associated with shorter reactivated structures (e.g., Horton et al., 2022; Jordan et al., 1983). Instead of a broad region of consistently sloping structural topography, as in orogenic wedges associated with thin-skinned fold-and-thrust belts, rock uplift along these structures tends to be disparate in space and time, leading to the formation of fault scarps and discrete ranges of limited along-strike extent (Figueroa et al., 2021; Hilley et al., 2005; Ramos et al., 2006; Strecker et al., 2012), whose bounding faults generate earthquakes of small to medium magnitude (Alvarado & Ramos, 2011; Campbell et al., 2019; Costa et al., 2020).

In the Santa Bárbara System, many small- to medium-magnitude earthquakes were recorded in previous decades (e.g., INPRES, 2021). A prominent recent example is the 2015 El Galpón earthquake in the northern sector of the Metán Basin (Figure 1), with a moment magnitude of Mw 5.8 and an estimated hypocenter depth of 17 km. In addition, two earthquakes of magnitude Mw 5.6 and Mw 5.0 occurred at a depth of approximately 10 km along the Iglesia (2) and San Pedro (12) faults in December 2021 and January 2022, respectively. Historical seismicity records date back to 1692, when an earthquake in the Metán Basin with an estimated Mw 7 devastated the Spanish colonial settlement of El Esteco (INPRES, 2012, 2015, 2019; USGS, 2015; Zossi, 1979). Other historical earthquakes near the Candelaria Range occurred in 1826 (Trancas, Mw 6.5), 1927 (Rosario de la Frontera, Mw 6.1), 1931 (El Naranjo, Mw 6.3), and 1948 (Anta, Mw 6.9) (Ortíz et al., 2022; Zossi, 1979).

Considering the seismic activity in the Santa Bárbara System, the existence of Quaternary faults and folds and ubiquitous geomorphological indicators of Quaternary tectonic activity, it can be inferred that ground-rupturing earthquakes contributed to the formation of the observed fault scarps and deformed alluvial-fan terraces (Arnous et al., 2020). However, it cannot be ruled out that some of these structures experienced continuous aseismic creep or frequent, small-magnitude ruptures that accumulated slip over time. These uncertainties may be particularly relevant for those fault scarps that were generated by flexural slip in the sedimentary cover rocks. Despite their pronounced scarp morphology, there is currently no reliable information available to confirm whether or not these faults may have caused significant earthquakes. Although there is uncertainty in many flexural-slip fault settings regarding seismogenic faulting along bedding planes, there are nevertheless examples of flexural-slip faults and folds that are associated with seismogenic slip. For example, the Seattle Fault in the western U.S. is a flexural-slip fault that has triggered Mw 5–6 earthquakes at depths between 5 and 8 km (e.g., Kelsey et al., 2008). The setting of the Seattle Fault resembles that of the eastern part of the Candelaria Range, where the El Quemado (10) and Copo Quile (11) faults ruptured the surface in the past (Figure 7), although further paleoseismological studies are needed to unambiguously confirm such a scenario.

Although Yeats et al. (1981) suggested that faults parallel to bedding may generate earthquakes without an external trigger mechanism from adjacent, deeper faults (review in Kelsey et al. (2008)), geological evidence from other tectonically active regions suggests that flexural-slip faults may be activated co-seismically during rupture of linked, deeper-seated crustal structures (e.g., Hull, 1990; Treiman, 1995; Yeats, 2000). For example, the 1981 Mw 2.5 Lompac earthquake of California, U.S. (Yerkes et al., 1983), the 1980 Mw 7.3 El Asnam earthquake in Algeria (Philip & Meghraoui, 1983), the Mw 6.6 2008 Nura earthquake in Kyrgyzstan (Patyniak, 2022; Patyniak et al., 2021), and the Mw 7.0 1944 San Juan earthquake in Argentina (Rockwell et al., 2014) may belong to this group of seismogenic faults. In all of these cases, it has been suggested that rupture on a reverse fault at middle to upper crustal levels may have triggered movement on shallow-seated, bedding-parallel flexural-slip faults. In addition, InSAR data presented by Kaneko et al. (2015) indicate that motion on flexural-slip faults can be triggered by the passage of seismic waves resulting from nearby large earthquakes, and thus slip along these structures could indeed occur co-seismically and cause surface rupture. In the context of these other examples where surface rupture occurred during flexural-slip deformation, the Arias (9), Barba Yaco (8), and San Esteban (7) faults are interpreted as flexural-slip faults that are rooted in incompetent strata of the Metán and Jujuy subgroups. These structures have the potential to be activated during medium- and large-magnitude earthquakes associated with deeper-seated, kinematically linked neighboring faults. Both, first-order faults (Candelaria and El Brete faults) and second-order faults (e.g., the blind fault underlying the El Arenal Anticline) represent potential seismogenic structures that can trigger ground-rupturing earthquakes.

7. Conclusions

The broken-foreland province of the Santa Bárbara System in northwestern Argentina exhibits a complex, spatially and temporally disparate structural framework of faults that are rooted at different depths of crustal detachments. While earlier studies had identified detachments at depths ranging from 10 km in the northern Santa Bárbara System to 25–40 km in the southern sectors, our structural model based on the integration of seismic reflection data, field observations, and kinematic modeling determines a first-order detachment level at approximately 23 km depth. This interpretation is supported by thermomechanical models and the distribution of earthquake hypocenters. Second-order faults have developed in response to contractional deformation within basins adjacent to reverse-fault bounded uplifts, with a detachment level located in the contact zone between sedimentary cover strata and metamorphic basement at a depth of 3–4 km.

Deformation in the Santa Bárbara System is strongly linked to the inversion of Cretaceous extensional faults. Total horizontal shortening in the central Santa Bárbara System is approximately 18.4 km and distributed among several structures, some of which have are still active today. However, analogous to the deformation observed in the adjacent Eastern Cordillera, some structures may have formed through reactivation of inherited basement heterogeneities. However, the exact role of inherited basement structures in guiding Cenozoic contractional reactivation remains the subject of ongoing research. A third group of neotectonic faults is associated with contractional thin-skinned deformation during flexural-slip faulting in the piedmonts of the broken-foreland ranges, which is well expressed geomorphically by linear fault scarps and pronounced drainage anomalies. Although these bedding-parallel structures have no link to deep-seated structures in the basement, they may be subjected to creep in response to medium- and large-magnitude earthquakes that rupture deeper structures in the basement.

Data Availability Statement

All the data and software used in this study are fully accessible through the text, figures, and Supporting Information S1. Specifically, the earthquake data (Zeckra, 2020; Zeckra & Krüger, 2023) featured in Figure 7 is retrievable from the ISC Seismological Data set Repository at https://doi.org/10.31905/YTIR1IED. The GPS-velocity data shown in Figure 7 originates from the works of McFarland et al. (2017) and Figueroa et al. (2021). Please note that access to the reprocessed seismic data and well-log information is restricted and can only be granted upon submitting a formal request to the Secretaría de Minería y Energía of the Province of Salta.

Acknowledgments
This research was funded by the German Research Foundation (DFG) Grant STR373/34-1 to M. Strecker and the Brandenburg Ministry of Sciences, Research and Cultural Affairs, Germany, within the framework of the International Research Training Group IGK2018 SuRfAce processes, Tectonics and Georesources: The Andean foreland basin of Argentina (StRATEGy). We also thank the German-Argentine University Network (DAHZ/CUAA; grant to M. Strecker and A. Gutierrez: *Riesgos Naturales*), the DAAD (Deutscher Akademischer Austauschdienst) and CONICET of Argentina for their funding and support of A. Arnous and L. Giambiagi. We express gratitude to the Secretaría de Minería y Energía of the Province of Salta for providing the seismic reflection data. We are indebted to G. Aranda and R. Alonso for fruitful discussions. Open Access funding enabled and organized by Projekt DEAL.

References

Allmendinger, R. W., Ramos, V. A., Jordan, T. E., Palma, M., & Isacks, B. L. (1983). Paleogeography and Andean structural geometry, northwest Argentina. *Tectonics*, *2*(1), 1–16. https://doi.org/10.1029/TC002i001p00001

Alvarado, P., & Ramos, V. A. (2011). Earthquake deformation in the northwestern Sierras Pampeanas of Argentina based on seismic waveform modelling. *Journal of Geodynamics*, *51*(4), 205–218. https://doi.org/10.1016/j.jog.2010.08.002

Arnous, A., Zeckra, M., Venerdini, A., Alvarado, P., Arrowsmith, R., Guillemoteau, J., et al. (2020). Neotectonic activity in the low-strain broken foreland (Santa Bárbara System) of the north-western Argentinean Andes (26°S). *Lithosphere*, *2020*(1). https://doi.org/10.2113/2020/8888588

Arrowsmith, J. R., Crosby, C. J., Korzhenkov, A. M., Mamyrov, E., Povolotskaya, I., Guralnik, B., & Landgraf, A. (2017). Surface rupture of the 1911 Kebin (Chon–Kemin) earthquake, northern Tien Shan, Kyrgyzstan. In A. Landgraf, S. Kübler, E. Hintersberger, & S. Stein (Eds.), *Seismicity, fault rupture and earthquake hazards in slowly deforming regions* (Vol. 432, pp. 233–253). Geological Society of London. https://doi.org/10.1144/sp432.10

Baby, P., Rochat, P., Mascle, G., & Hérail, G. (1997). Neogene shortening contribution to crustal thickening in the back arc of the Central Andes. *Geology*, *25*(10), 883–886. https://doi.org/10.1130/0091-7613(1997)025<0883:NSCTCT>2.3.CO;2

Barcelona, H., Peri, G., Tobal, J., Sagripanti, L., & Favetto, A. (2014). Tectonic activity revealed by morphostructural analysis: Development of the Sierra de la Candelaria range, northwestern Argentina. *Journal of South American Earth Sciences*, *56*, 376–395. https://doi.org/10.1016/j.jsames.2014.10.002

Bossi, G. E. (1969). Geología y estratigrafía del sector sur del valle de Choromoro. *Acta Geológica Lilloana*, *10*, 17–64.

Brooks, B. A., Bevis, M., Whipple, K., Arrowsmith, J. R., Foster, J., Zapata, T., et al. (2011). Orogenic-wedge deformation and potential for great earthquakes in the Central Andean backarc. *Nature Geoscience*, *4*(6), 380–383. https://doi.org/10.1038/ngeo1143

Cahill, T., & Isacks, B. L. (1992). Seismicity and shape of the subducted Nazca Plate. *Journal of Geophysical Research*, *97*(B12), 17503–17529. https://doi.org/10.1029/92JB00493

Campbell, G. E., Walker, R. T., Abdrakhmatov, K., Carolin, S., Carr, A. S., Elliott, J. R., et al. (2019). Rapid late Quaternary slip, repeated prehistoric earthquake rupture, and widespread landsliding associated with the Karakudzhur Thrust, Central Kyrgyz Tien Shan. *Tectonics*, *38*(11), 3740–3764. https://doi.org/10.1029/2018tc005433

Carrapa, B., Trimble, J. D., & Stockli, D. F. (2011). Patterns and timing of exhumation and deformation in the Eastern Cordillera of NW Argentina revealed by (U-Th)/He thermochronology. *Tectonics*, *30*(3), TC3003. https://doi.org/10.1029/2010TC002707

Carrera, N., Muñoz, J. A., Sàbat, F., Mon, R., & Roca, E. (2006). The role of inversion tectonics in the structure of the Cordillera Oriental (NW Argentinean Andes). *Journal of Structural Geology*, *28*(11), 1921–1932. https://doi.org/10.1016/j.jsg.2006.07.006

Costa, C., Alvarado, A., Audemard, F., Audin, L., Benavente, C., Bezerra, F. H., et al. (2020). Hazardous faults of South America; compilation and overview. *Journal of South American Earth Sciences*, *104*, 102837. https://doi.org/10.1016/j.jsames.2020.102837

Costa, C., Rockwell, T., Paredes, J., & Gardini, C. (1999). Quaternary deformations and seismic hazard at the Andean orogenic front (31°–33°, Argentina): A paleoseismological perspective. In *Paper presented at 4th ISAG*. Universität Göttingen.

Costa, C. H., Owen, L. A., Ricci, W. R., Johnson, W. J., & Halperin, A. D. (2018). Holocene activity and seismogenic capability of intraplate thrusts: Insights from the Pampean Ranges, Argentina. *Tectonophysics*, *737*, 57–70. https://doi.org/10.1016/j.tecto.2018.05.002

Cristallini, E., Cominguez, A. H., & Ramos, V. A. (1997). Deep structure of the Metan-Guachipas region: Tectonic inversion in northwestern Argentina. *Journal of South American Earth Sciences*, *10*(5–6), 403–421. https://doi.org/10.1016/S0895-9811(97)00026-6

Cristallini, E., Cominguez, A. H., Ramos, V. A., & Mercerat, E. D. (2004). Basement double-wedge thrusting in the northern Sierras Pampeanas of Argentina (27°S)—Constraints from deep seismic reflection. In K. R. McClay (Ed.), *Thrust tectonics and hydrocarbon systems* (Vol. 82, pp. 65–90). AAPG Memoir. https://doi.org/10.1306/M82813C5

DeCelles, P. G. (2012). Foreland basin systems revisited: Variations in response to tectonic settings. In C. Busby, & A. Azor (Eds.), *Tectonics of sedimentary basins: Recent advances* (pp. 405–426). John Wiley & Sons, Ltd. https://doi.org/10.1002/9781444347166.ch20

Deeken, A., Sobel, E. R., Coutand, I., Haschke, M., Riller, U., & Strecker, M. R. (2006). Development of the southern Eastern Cordillera, NW Argentina, constrained by apatite fission track thermochronology: From early Cretaceous extension to middle Miocene shortening. *Tectonics*, *25*(6), TC6003. https://doi.org/10.1029/2005TC001894

del Papa, C., Payrola, P., Pingel, H., Hongn, F., Do Campo, M., Sobel, E. R., et al. (2021). Stratigraphic response to fragmentation of the Miocene Andean foreland basin, NW Argentina. *Basin Research*, *33*(6), 2914–2937. https://doi.org/10.1111/bre.12589

Dunn, J. F., Hartshorn, K. G., & Hartshorn, P. W. (1995). Structural styles and hydrocarbon potential of the sub-Andean thrust belt of southern Bolivia. In A. J. Tankard, R. Suárez-Soruco, & H. J. Welsink (Eds.), *Petroleum basins of South America* (Vol. 62, pp. 523–543). American Association of Petroleum Geologists. https://doi.org/10.1306/m62593c27

Echavarria, L., Hernández, R., Allmendinger, R., & Reynolds, J. (2003). Subandean thrust and fold belt of northwestern Argentina: Geometry and timing of the Andean evolution. *AAPG Bulletin*, *87*(6), 965–985. https://doi.org/10.1306/01200300196

England, P., & Jackson, J. (2011). Uncharted seismic risk. *Nature Geoscience*, *4*(6), 348–349. https://doi.org/10.1038/ngeo1168

Erslev, E. A. (1991). Trishear fault-propagation folding. *Geology*, *19*(6), 617. https://doi.org/10.1130/0091-7613(1991)019<0617:TFPF>2.3.CO;2

Figueroa, S., Weiss, J. R., Hongn, F., Pingel, H., Escalante, L., Elías, L., et al. (2021). Late Pleistocene to recent deformation in the thick-skinned fold-and-thrust belt of northwestern Argentina (Central Calchaquí Valley, 26°S). *Tectonics*, *40*(1), e2020TC006394. https://doi.org/10.1029/2020TC006394

García, V. H., Hongn, F., & Cristallini, E. O. (2013). Late Miocene to recent morphotectonic evolution and potential seismic hazard of the northern Lerma valley: Clues from Lomas de Medeiros, Cordillera Oriental, NW Argentina. *Tectonophysics*, *608*, 1238–1253. https://doi.org/10.1016/j.tecto.2013.06.021

García, V. H., Hongn, F., Yagupsky, D., Pingel, H., Kinnaird, T., Winocur, D., et al. (2019). Late Quaternary tectonics controlled by fault reactivation. Insights from a local transpressional system in the intermontane Lerma valley, Cordillera Oriental, NW Argentina. *Journal of Structural Geology*, *128*, 103875. https://doi.org/10.1016/j.jsg.2019.103875

Gebhard, J. A., Guidice, A. R., & Gascon, J. O. (1974). Geología de la comarca entre el Río Juramento y Arroyo las Tortugas, provincias de Salta y Jujuy. *Revista de la Asociación Geológica Argentina*, *29*, 359–375.

Giambiagi, L., Tassara, A., Echaurren, A., Julve, J., Quiroga, R., Barrionuevo, M., et al. (2022). Crustal anatomy and evolution of a subduction-related orogenic system: Insights from the southern Central Andes (22-35°S). *Earth-Science Reviews*, *232*, 104138. https://doi.org/10.1016/j.earscirev.2022.104138

Grier, M. E., Salfity, J. A., & Allmendinger, R. W. (1991). Andean reactivation of the Cretaceous Salta rift, northwestern Argentina. *Journal of South American Earth Sciences*, *4*(4), 351–372. https://doi.org/10.1016/0895-9811(91)90007-8

Hain, M. P., Strecker, M. R., Bookhagen, B., Alonso, R. N., Pingel, H., & Schmitt, A. K. (2011). Neogene to Quaternary broken foreland formation and sedimentation dynamics in the Andes of NW Argentina (25°S). *Tectonics*, *30*(2), TC2006. https://doi.org/10.1029/2010tc002703

Hayes, G. P., Moore, G. L., Portner, D. E., Hearne, M., Flamme, H., Furtney, M., & Smoczyk, G. M. (2018). Slab2, a comprehensive subduction zone geometry model. *Science*, *362*(6410), 58–61. https://doi.org/10.1126/science.aat472

Hilley, G. E., Blisniuk, P. M., & Strecker, M. R. (2005). Mechanics and erosion of basement cored uplift provinces. *Journal of Geophysical Research*, *110*(B12), B12409. https://doi.org/10.1029/2005JB003704

Hongn, F., Mon, R., Petrinovic, I., Del Papa, C., & Powell, J. (2010). Inversión y reactivación tectónicas cretácicocenozoicas en el Noroeste Argentino: influencia de las heterogeneidades del basamento neoproterozoico-paleozoico inferior. *Revista de la Asociación Geológica Argentina*, *66*(1–2), 38–53. Retrieved from https://revista.geologica.org.ar/raga/article/view/841

Hongn, F. D., & Riller, U. (2007). Tectonic evolution of the western margin of Gondwana inferred from syntectonic emplacement of Paleozoic granitoid plutons in northwest Argentina. *The Journal of Geology*, *115*(2), 163–180. https://doi.org/10.1086/510644

Horton, B. K., Capaldi, T. N., & Perez, N. D. (2022). The role of flat slab subduction, ridge subduction, and tectonic inheritance in Andean deformation. *Geology*, *50*(9), 1007–1012. https://doi.org/10.1130/G50094.1

Hull, A. G. (1990). Tectonics of the 1931 Hawke's Bay earthquake. *New Zealand Journal of Geology and Geophysics*, *33*(2), 309–320. https://doi.org/10.1080/00288306.1990.10425689

Iaffa, D. N., Sàbat, F., Muñoz, J. A., & Carrera, N. (2013). Basin fragmentation controlled by tectonic inversion and basement uplift in Sierras Pampeanas and Santa Bárbara System, northwest Argentina. In M. Nemčok, A. Mora, & J. W. Cosgrove (Eds.), *Thick-skin-dominated orogens: From initial inversion to full accretion* (Vol. 377(1), pp. 101–117). Geological Society of London. https://doi.org/10.1144/sp377.13

Iaffa, D. N., Sàbat, F., Muñoz, J. A., Mon, R., & Gutierrez, A. A. (2011). The role of inherited structures in a foreland basin evolution. The Metán Basin in NW Argentina. *Journal of Structural Geology*, *33*(12), 1816–1828. https://doi.org/10.1016/j.jsg.2011.09.005

Ibarra, F., Liu, S., Meeßen, C., Prezzi, C., Bott, J., Scheck-Wenderoth, M., & Strecker, M. (2019). 3D data-derived lithospheric structure of the Central Andes and its implications for deformation: Insights from gravity and geodynamic modelling. *Tectonophysics*, *766*, 453–468. https://doi.org/10.1016/j.tecto.2019.06.025

Ibarra, F., Prezzi, C. B., Bott, J., Scheck-Wenderoth, M., & Strecker, M. R. (2021). Distribution of temperature and strength in the Central Andean lithosphere and its relationship to seismicity and active deformation. *Journal of Geophysical Research: Solid Earth*, *126*(5), e2020JB021231. https://doi.org/10.1029/2020JB021231

Instituto Nacional de Prevencion Sismica, INPRES. (2012). Listado de terremotos históricos. On-line catalogue. Retrieved from http://contenidos.inpres.gob.ar/sismologia/historicos

Instituto Nacional de Prevencion Sismica, INPRES. (2015). Listado de terremotos históricos. On-line catalogue.

Instituto Nacional de Prevencion Sismica, INPRES. (2019). Listado de terremotos históricos. On-line catalogue.

Instituto Nacional de Prevencion Sismica, INPRES. (2021). Listado de terremotos históricos. On-line catalogue.

Instituto Nacional de Prevencion Sismica, INPRES. (2022). Listado de terremotos históricos. On-line catalogue.

Invernizzi, C., Pierantoni, P. P., Chiodi, A., Maffucci, R., Corrado, S., Baez, W., et al. (2014). Preliminary assessment of the geothermal potential of Rosario de la Frontera area (Salta, NW Argentina): Insight from hydro-geological, hydro-geochemical and structural investigations. *Journal of South American Earth Sciences*, *54*, 20–36. https://doi.org/10.1016/j.jsames.2014.04.003

Jordan, T. E., & Allmendinger, R. W. (1986). The Sierras Pampeanas of Argentina; a modern analogue of Rocky Mountain foreland deformation. *American Journal of Science*, *286*(10), 737–764. https://doi.org/10.2475/ajs.286.10.737

Jordan, T. E., Isacks, B. L., Allmendinger, R. W., Brewer, J. A., Ramos, V. A., & Ando, C. J. (1983). Andean tectonics related to geometry of subducted Nazca plate. *Geological Society of America Bulletin*, *94*(3), 341–361. https://doi.org/10.1130/0016-7606(1983)94<341:atrtgo>2.0.co;2

Kaneko, Y., Hamling, I. J., Van Dissen, R. J., Motagh, M., & Samsonov, S. V. (2015). InSAR imaging of displacement on flexural-slip faults triggered by the 2013 Mw 6.6 Lake Grassmere earthquake, Central New Zealand. *Geophysical Research Letters*, *42*(3), 781–788. https://doi.org/10.1002/2014GL062767

Kelsey, H. M., Sherrod, B. L., Nelson, A. R., & Brocher, T. M. (2008). Earthquakes generated from bedding plane-parallel reverse faults above an active wedge thrust, Seattle fault zone. *Geological Society of America Bulletin*, *120*(11–12), 1581–1597. https://doi.org/10.1130/B26282.1

Kley, J., & Monaldi, C. R. (2002). Tectonic inversion in the Santa Barbara System of the central Andean foreland thrust belt, northwestern Argentina. *Tectonics*, *21*(6), 1061. https://doi.org/10.1029/2002TC902003

Kley, J., Monaldi, C. R., & Salfity, J. A. (1999). Along-strike segmentation of the Andean foreland: Causes and consequences. *Tectonophysics*, *301*(1–2), 75–94. https://doi.org/10.1016/S0040-1951(98)90223-2

Kley, J., Rossello, E. A., Monaldi, C. R., & Habighorst, B. (2005). Seismic and field evidence for selective inversion of Cretaceous normal faults, Salta rift, northwest Argentina. *Tectonophysics*, *399*(1–4), 155–172. https://doi.org/10.1016/j.tecto.2004.12.020

Kley, J., & Voigt, T. (2008). Late Cretaceous intraplate thrusting in central Europe: Effect of Africa-Iberia-Europe convergence, not Alpine collision. *Geology*, *36*(11), 839–842. https://doi.org/10.1130/G24930A.1

Lacombe, O., & Bellahsen, N. (2016). Thick-skinned tectonics and basement-involved fold–thrust belts: Insights from selected Cenozoic orogens. *Geological Magazine*, *153*(5–6), 763–810. https://doi.org/10.1017/S0016756816000078

Landgraf, A., Kuebler, S., Hintersberger, E., & Stein, S. (2017). Active tectonics, earthquakes and palaeoseismicity in slowly deforming continents. In A. Landgraf, S. Kübler, E. Hintersberger, & S. Stein (Eds.), *Seismicity, fault rupture and earthquake hazards in slowly deforming regions* (Vol. 432, pp. 1–12). Geological Society of London. https://doi.org/10.1144/sp432.13

Liu, S., Sobolev, S. V., Babeyko, A. Y., & Pons, M. (2022). Controls of the foreland deformation pattern in the orogen-foreland shortening system: Constraints from high-resolution geodynamic models. *Tectonics*, *41*(2), e2021TC007121. https://doi.org/10.1029/2021TC007121

Löbens, S., Sobel, E. R., Bense, F. A., Wemmer, K., Dunkl, I., & Siegesmund, S. (2013a). Refined exhumation history of the northern Sierras Pampeanas, Argentina. *Tectonics*, *32*(3), 453–472. https://doi.org/10.1002/tect.20038

Madritsch, H., Schmid, S. M., & Fabbri, O. (2008). Interactions between thin-and thick-skinned tectonics at the northwestern front of the Jura fold-and-thrust belt (eastern France). *Tectonics*, *27*(5), TC5005. https://doi.org/10.1029/2008TC002282

Maffucci, R., Bigi, S., Corrado, S., Chiodi, A., Di Paolo, L., Giordano, G., & Invernizzi, C. (2015). Quality assessment of reservoirs by means of outcrop data and "discrete fracture network" models: The case history of Rosario de La Frontera (NW Argentina) geothermal system. *Tectonophysics*, *647*, 112–131. https://doi.org/10.1016/j.tecto.2015.02.01

Marquillas, R. A., Del Papa, C., & Sabino, I. F. (2005). Sedimentary aspects and paleoenvironmental evolution of a rift basin: Salta Group (Cretaceous–Paleogene), northwestern Argentina. *International Journal of Earth Sciences*, *94*(1), 94–113. https://doi.org/10.1007/s00531-004-0443-2

Marshak, S., Karlstrom, K., & Timmons, J. M. (2000). Inversion of Proterozoic extensional faults: An explanation for the pattern of Laramide and Ancestral Rockies intracratonic deformation, United States. *Geology*, *28*(8), 735–738. https://doi.org/10.1130/0091-7613(2000)28<735:IOPEFA>2.0.CO;2

McFarland, P. K., Bennett, R. A., Alvarado, P., & DeCelles, P. G. (2017). Rapid geodetic shortening across the Eastern Cordillera of NW Argentina observed by the Puna-Andes GPS array. *Journal of Geophysical Research: Solid Earth*, *122*(10), 8600–8623. https://doi.org/10.1002/2017JB014739

McQuarrie, N., Horton, B. K., Zandt, G., Beck, S., & DeCelles, P. G. (2005). Lithospheric evolution of the Andean fold–thrust belt, Bolivia, and the origin of the Central Andean Plateau. *Tectonophysics*, *399*(1–4), 15–37. https://doi.org/10.1016/j.tecto.2004.12.013

Medwedeff, D. A. (1989). Growth fault-bend folding at Southeast Lost Hills, SanJoaquin Valley, California. *AAPG Bulletin*, *73*. https://doi.org/10.1306/703C9AE6-1707-11D7-8645000102C1865D

Mon, R., & Gutiérrez, A. A. (2007). Estructura del extremo sur del sistema subandino (provincias de Salta, Santiago del Estero y Tucumán). *Revista de la Asociación Geológica Argentina*, *62*(1), 62–68. Retrieved from https://revista.geologica.org.ar/raga/article/view/1146

Mon, R., & Hongn, F. (1991). The structure of the Precambrian and Lower Paleozoic basement of the Central Andes between 22° and 32°S. Lat. *Geologische Rundschau*, *80*(3), 745–758. https://doi.org/10.1007/BF01803699

Mon, R., & Salfity, J. A. (1995). Tectonic evolution of the Andes of northern Argentina. In A. J. Tankard, R. Suárez-Soruco, & H. J. Welsink (Eds.), *Petroleum basins of South America* (Vol. 62, pp. 269–283). American Association of Petroleum Geologists. https://doi.org/10.1306/m62593c12

Mora, A., Parra, M., Strecker, M. R., Kammer, A., Dimaté, C., & Rodríguez, F. (2006). Cenozoic contractional reactivation of Mesozoic extensional structures in the Eastern Cordillera of Colombia. *Tectonics*, *25*(2). https://doi.org/10.1029/2005TC001854

Mortimer, E., Carrapa, B., Coutand, I., Schoenbohm, L., Sobel, E. R., Sosa Gomez, J., & Strecker, M. R. (2007). Fragmentation of a foreland basin in response to out-of-sequence basement uplifts and structural reactivation: El Cajón–Campo del Arenal basin, NW Argentina. *Geological Society of America Bulletin*, *119*(5–6), 637–653. https://doi.org/10.1130/B25884.1

Mugnier, J.-L., Gajurel, A., Huyghe, P., Jayangondaperumal, R., Jouanne, F., & Upreti, B. (2013). Structural interpretation of the great earthquakes of the last millennium in the central Himalaya. *Earth-Science Reviews*, *127*, 30–47. https://doi.org/10.1016/j.earscirev.2013.09.003

Oliver, J. (1986). Fluids expelled tectonically from orogenic belts: Their role in hydrocarbon migration and other geologic phenomena. *Geology*, *14*(2), 99–102. https://doi.org/10.1130/0091-7613(1986)14<99:FETFOB>2.0.CO;2

Ortiz, G., Saez, M., Alvarado, P., Rivas, C., García, V., Alonso, R., & Zullo, F. M. (2022). Seismotectonic characterization of the 1948 (MW 6.9) Anta earthquake, Santa Bárbara System, Central Andes broken foreland of northwestern Argentina. *Journal of South American Earth Sciences*, *116*, 103822. https://doi.org/10.1016/j.jsames.2022.103822

Padula, E. L., Rolleri, E. O., Mingramm, A. R. G., Roque, P. C., Flores, M. A., & Baldis, B. A. (1967). Devonian of Argentina. In D. H. Oswald (Ed.), *International symposium on the Devonian system, Calgary, 1967* (Vol. 2, pp. 165–199). Alberta Society of Petroleum Geologists.

Patyniak, M. (2022). *Seismotectonic segmentation, paleoearthquakes and style of deformation along the northern Pamir thrust system, South Kyrgyzstan*. PhD thesis. (p. 165). Universität Potsdam.

Patyniak, M., Landgraf, A., Dzhumabaeva, A., Abdrakhmatov, K. E., Rosenwinkel, S., Korup, O., et al. (2017). Paleoseismic record of three Holocene earthquakes rupturing the Issyk-Ata Fault near Bishkek, North Kyrgyzstan. *Bulletin of the Seismological Society of America*, *107*(6), 2721–2737. https://doi.org/10.1785/0120170083

Patyniak, M., Landgraf, A., Dzhumabaeva, A., Baikulov, S., Williams, A. M., Weiss, J. R., et al. (2021). The Pamir Frontal Thrust Fault: Holocene full-segment ruptures and implications for complex segment interactions in a continental collision zone. *Journal of Geophysical Research: Solid Earth*, *126*(12), e2021JB022405. https://doi.org/10.1029/2021jb022405

Payrola, P., del Papa, C., Aramayo, A., Pingel, H., Hongn, F., Sobel, E. R., et al. (2020). Episodic out-of-sequence deformation promoted by Cenozoic fault reactivation in NW Argentina. *Tectonophysics*, *776*, 228276. https://doi.org/10.1016/j.tecto.2019.228276

Pearson, D. M., Kapp, P., DeCelles, P. G., Reiners, P. W., Gehrels, G. E., Ducea, M. N., & Pullen, A. (2013). Influence of pre-Andean crustal structure on Cenozoic thrust belt kinematics and shortening magnitude: Northwestern Argentina. *Geosphere*, *9*(6), 1766–1782. https://doi.org/10.1130/ges00923.1

Pfiffner, O. A. (2017). Thick-skinned and thin-skinned tectonics: A global perspective. *Geosciences*, *7*(3), 71. https://doi.org/10.3390/geosciences7030071

Philip, H., & Meghraoui, M. (1983). Structural analysis and interpretation of the surface deformations of the El Asnam earthquake of October 10, 1980. *Tectonics*, *2*(1), 17–49. https://doi.org/10.1029/TC002i001p00017

Pingel, H., Alonso, R. N., Bookhagen, B., Cottle, J. M., Mulch, A., Rohrmann, A., & Strecker, M. R. (2023). Miocene surface uplift and orogenic evolution of the southern Andean Plateau (central Puna), northwestern Argentina. *Proceedings of the National Academy of Sciences of the United States of America*, *120*(42). https://doi.org/10.1073/pnas.2303964120

Pingel, H., Deeken, A., Coutand, I., Alonso, R. N., Riller, U., Sobel, E. R., et al. (2023). Cenozoic exhumation and deformation of the intermontane Pastos Chicos Basin in the southern Central Andes: Implications for the tectonic evolution of the Andean Plateau (Puna) and the Eastern Cordillera between 23° and 24°S, NW Argentina. *Tectonics*, *42*(2), e2022TC007487. https://doi.org/10.1029/2022tc007487

Pons, M., Rodriguez Piceda, C., Sobolev, S. V., Scheck-Wenderoth, M., & Strecker, M. R. (2023). Localization of deformation in a non-collisional subduction orogen: The roles of dip geometry and plate strength on the evolution of the broken Andean foreland, Sierras Pampeanas, Argentina. *Tectonics*, *42*(8), e2023TC007765. https://doi.org/10.1029/2023TC007765

Ramos, V. A., Alonso, R. N., & Strecker, M. R. (2006). Estructura y neotectónica de Las Lomas de Olmedo, zona de transición entre los Sistemas Subandino y de Santa Bárbara, provincia de Salta. *Revista de la Asociación Geológica Argentina*, *61*(4), 579–588. Retrieved from https://revista.geologica.org.ar/raga/article/view/1357

Ramos, V. A., Cristallini, E. O., & Pérez, D. J. (2002). The Pampean flat-slab of the Central Andes. *Journal of South American Earth Sciences*, *15*(1), 59–78. https://doi.org/10.1016/S0895-9811(02)00006-8

Reynolds, J. H., Galli, C. I., Hernández, R. M., Idleman, B. D., Kotila, J. M., Hilliard, R. V., & Naeser, C. W. (2000). Middle Miocene tectonic development of the transition zone, Salta Province, northwest Argentina: Magnetic stratigraphy from the Metan Subgroup, Sierra de Gonzalez. *Geological Society of America Bulletin*, *112*(11), 1736–1751. https://doi.org/10.1130/0016-7606(2000)112%3C1736:MMTDOT%3E2.0.CO;2

Reynolds, J. H., Idleman, B. D., Hernández, R. M., & Naeser, C. W. (1994). Preliminary chronostratigraphic constraints on Neogene tectonic activity in the Eastern Cordillera and Santa Bárbara System, Salta province, NW Argentina. *Geological Society of America Abstracts with Programs*, *26*(7), A–503.

Ricci, H., & Villanueva, A. (1969). Sobre la presencia de Paleozoico inferior en la Sierra de la Candelaria (Prov. de Salta). *Acta Geológica Lilloana*, *10*(1), 1–16.

Rockwell, T. K., Ragona, D. E., Meigs, A. J., Owen, L. A., Costa, C. H., & Ahumada, E. A. (2014). Inferring a thrust-related earthquake history from secondary faulting: A long rupture record of La Laja Fault, San Juan, Argentina. *Bulletin of the Seismological Society of America*, *104*(1), 269–284. https://doi.org/10.1785/0120110080

Rodriguez Piceda, C., Gao, Y.-J., Cacace, M., Scheck-Wenderoth, M., Bott, J., Strecker, M., & Tilmann, F. (2023). The influence of mantle hydration and flexure on slab seismicity in the southern Central Andes. *Communications Earth & Environment*, *4*(1), 79. https://doi.org/10.1038/s43247-023-00729-1

Russo, A., & Serraiotto, A. (1978). Contribucion al conocimiento de la estratigrafia Terciaria en el noroeste argentino. *Actas del VII Congreso Geológico Argentino*, *1*, 715–730.

Salfity, J. A., & Marquillas, R. A. (1994). Tectonic and sedimentary evolution of the Cretaceous-Eocene Salta group basin, Argentina. In J. A. Salfity (Ed.), *Cretaceous tectonics of the Andes. Earth evolution sciences* (pp. 266–315). Vieweg+Teubner Verlag. https://doi.org/10.1007/978-3-322-85472-8_6

Salfity, J. A., & Monaldi, C. R. (2006). *Hoja Geológica 2566-IV, Metán, Provincia de Salta (Boletín 352)* (p. 74). Instituto de Geología y Recursos Minerales, Servicio Geológico Minero Argentino.

Sanchez, G., Recio, R., Marcuzzi, O., Moreno, M., Araujo, M., Navarro, C., et al. (2013). The Argentinean national network of seismic and strong-motion stations. *Seismological Research Letters*, *84*(5), 729–736. https://doi.org/10.1785/0220120045

Scholz, C. H. (2002). *The mechanics of earthquakes and faulting* (2nd ed., p. 471). Cambridge University Press. https://doi.org/10.1017/cbo9780511818516

Scott, C., Lohman, R., Pritchard, M., Alvarado, P., & Sánchez, G. (2014). Andean earthquakes triggered by the 2010 Maule, Chile (Mw 8.8) earthquake: Comparisons of geodetic, seismic and geologic constraints. *Journal of South American Earth Sciences*, *50*, 27–39. https://doi.org/10.1016/j.jsames.2013.12.001

Seagren, E. G., McMillan, M., & Schoenbohm, L. M. (2022). Tectonic control on drainage evolution in broken forelands: Examples from NW Argentina. *Tectonics*, *41*(1), e2020TC006536. https://doi.org/10.1029/2020TC006536

Seggiaro, R., Gallardo, E., Aguilera, N., Vitulli, N., Brandan, E., Bercheñi, V., et al. (2015). Modelo estructural del área termal de la Sierra La Candelaria, Departamento Rosario de la Frontera, Salta. *Revista de la Asociación Geológica Argentina*, *72*(2), 265–278.

Sobel, E. R., & Strecker, M. R. (2003). Uplift, exhumation and precipitation: Tectonic and climatic control of late Cenozoic landscape evolution in the northern Sierras Pampeanas, Argentina. *Basin Research*, *15*(4), 431–451. https://doi.org/10.1046/j.1365-2117.2003.00214.x

Stein, S. (2010). *Disaster deferred: How new science is changing our view of earthquake hazards in the Midwest* (p. 296). Columbia University Press.

Stein, S., & Mazzotti, S. (2007). Continental intaplate earthquakes: Science, hazard, and policy issue. *GSA Specimen Paper*, *425*, 397.

Strecker, M. R., Hilley, G. E., Bookhagen, B., & Sobel, E. R. (2012). Structural, geomorphic, and depositional characteristics of contiguous and broken foreland basins: Examples from the eastern flanks of the Central Andes in Bolivia and NW Argentina. In C. Busby, & A. Azor (Eds.), *Tectonics of sedimentary basins: Recent advances* (pp. 508–521). John Wiley & Sons, Ltd. https://doi.org/10.1002/9781444347166.ch25

Teixell, A., Arboleya, M., Julivert, M., & Charroud, M. (2003). Tectonic shortening and topography in the central High Atlas (Morocco). *Tectonics*, *22*(5), 1051. https://doi.org/10.1029/2002TC001460

Treiman, J. A. (1995). Surface faulting near Santa Clarita. In M. C. Woods, & W. R. Seiple (Eds.), *The Northridge, California, earthquake of 17 January 1994* (Vol. 116, pp. 103–110). California Department of Conservation, Division of Mines and Geology Special Publication.
Turner, J. C. (1960). Estratigrafía de la Sierra de Santa Victoria y adyacencias. *Boletin de la Academia Nacional de Clencias*, *42*, 163–206.
U.S. Geological Survey, USGS. (2015). Earthquake hazard program: U.S. geological survey database. Retrieved from https://earthquake.usgs.gov/earthquakes/eventpage/us10003pc9/executive
Weiss, J. R., Brooks, B. A., Arrowsmith, J. R., & Vergani, G. (2015). Spatial and temporal distribution of deformation at the front of the Andean orogenic wedge in southern Bolivia. *Journal of Geophysical Research: Solid Earth*, *120*(3), 1909–1931. https://doi.org/10.1002/2014JB011763
Weiss, J. R., Brooks, B. A., Foster, J. H., Bevis, M., Echalar, A., Caccamise, D., et al. (2016). Isolating active orogenic wedge deformation in the southern Subandes of Bolivia. *Journal of Geophysical Research: Solid Earth*, *121*(8), 6192–6218. https://doi.org/10.1002/2016jb013145
Wells, D. L., & Coppersmith, K. J. (1994). New empirical relationships among magnitude, rupture length, rupture width, rupture area, and surface displacement. *Bulletin of the Seismological Society of America*, *84*(4), 974–1002. https://doi.org/10.1785/bssa0840040974
Yeats, R. S. (2000). The 1968 Inangahua, New Zealand, and 1994 Northridge, California, earthquakes: Implications for northwest Nelson. *New Zealand Journal of Geology and Geophysics*, *43*(4), 587–599. https://doi.org/10.1080/00288306.2000.9514911
Yeats, R. S., Clark, M. N., Keller, E. A., & Rockwell, T. K. (1981). Active fault hazard in southern California: Ground rupture versus seismic shaking. *Geological Society of America Bulletin*, *92*(4), 189–196. https://doi.org/10.1130/0016-7606(1981)92<189:afhisc>2.0.co;2
Yerkes, R. F., Ellsworth, W. L., & Tinsley, J. C. (1983). Triggered reverse fault and earthquake due to crustal unloading, northwest Transverse Ranges, California. *Geology*, *11*(5), 287–291. https://doi.org/10.1130/0091-7613(1983)11%3C287:TRFAED%3E2.0.CO;2
Zapata, S., Sobel, E. R., Del Papa, C., & Glodny, J. (2020). Upper plate controls on the formation of broken foreland basins in the Andean retroarc between 26°S and 28°S: From Cretaceous rifting to Paleogene and Miocene broken foreland basins. *Geochemistry, Geophysics, Geosystems*, *21*(7), e2019GC008876. https://doi.org/10.1029/2019GC008876
Zeckra, M. (2020). *Seismological and seismotectonic analysis of the northwestern Argentine Central Andean foreland*. PhD thesis. (p. 120). Universität Potsdam. https://doi.org/10.25932/publishup-47324
Zeckra, M., & Krüger, F. (2023). Earthquake catalog of a temporary seismic network in NW Argentine Andean Foreland (FDSN code: 2S (2016-2017)) [Dataset]. *ISC Seismological Dataset Repository*. https://doi.org/10.31905/YTIR1IED
Zeckra, M., Krüger, F., Aranda-Viana, R. G., Hongn, F., Ibarra, F., Weiss, J., & Strecker, M. R. (2023). Seismotectonics of the thick-skinned Santa Bárbara System in northwestern Argentina: Implications for regional crustal rheology and structure. *ESS Open Archive*. https://doi.org/10.22541/essoar.168565411.14528155/v1
Zossi, M. M. (1979). *Sísmicidad y tectonica en los Andes del Norte Argentino*. (PhD thesis). (pp. 125). Universidad Nacional de Tucumán.

References From the Supporting Information

Aramayo, A. J., Hongn, F. D., & del Papa, C. E. (2017). Acortamiento Paleógeno en el tramo medio de los Valles Calchaquíes: depositación sintectónica de la Formación Quebrada de los Colorados. *Revista de la Asociación Geológica Argentina*, *74*(4), 524–536.
Carrapa, B., Adelmann, D., Hilley, G. E., Mortimer, E., Sobel, E. R., & Strecker, M. R. (2005). Oligocene range uplift and development of plateau morphology in the southern Central Andes. *Tectonics*, *24*(4). https://doi.org/10.1029/2004tc001762
Carrapa, B., & DeCelles, P. G. (2008). Eocene exhumation and basin development in the Puna of northwestern Argentina. *Tectonics*, *27*(1). https://doi.org/10.1029/2007tc002127
Coutand, I., Carrapa, B., Deeken, A., Schmitt, A. K., Sobel, E. R., & Strecker, M. R. (2006). Propagation of orographic barriers along an active range front: Insights from sandstone petrography and detrital apatite fission-track thermochronology in the intra- montane Angastaco basin, NW Argentina. *Basin Research*, *18*(1), 1–26. https://doi.org/10.1111/j.1365-2117.2006.00283.x
Coutand, I., Cobbold, P. R., Urreiztieta, M., Gautier, P., Chauvin, A., Gapais, D., et al. (2001). Style and history of Andean deformation, Puna Plateau, northwestern Argentina. *Tectonics*, *20*(2), 210–234. https://doi.org/10.1029/2000tc900031
del Papa, C., Hongn, F., Powell, J., Payrola, P., Do Campo, M., Strecker, M. R., et al. (2013). Middle Eocene-Oligocene broken-foreland evolution in the Andean Calchaqui Valley, NW Argentina: Insights from stratigraphic, structural and provenance studies. *Basin Research*, *25*(5), 574–593. https://doi.org/10.1111/bre.12018
Kraemer, B., Adelmann, D., Alten, M., Schnurr, W., Erpenstein, K., Kiefer, E., et al. (1999). Incorporation of the Paleogene foreland into the Neogene Puna Plateau: The Salar de Antofalla area, NW Argentina. *Journal of South American Earth Sciences*, *12*(2), 157–182. https://doi.org/10.1016/s0895-9811(99)00012-7
Löbens, S., Bense, F. A., Dunkl, I., Wemmer, K., Kley, J., & Siegesmund, S. (2013b). Thermochronological constraints of the exhumation and uplift of the Sierra de Pie de Palo, NW Argentina. *Journal of South American Earth Sciences*, *48*, 209–219. https://doi.org/10.1016/j.jsames.2013.09.005
McMillan, M., Schoenbohm, L. M., Tye, A., McMillan, M. F., & Zhou, R. (2022). Eocene to quaternary deformation of the southern Puna Plateau: Thermochronology, geochronology, and structural geology of an Andean Hinterland Basin (NW Argentina). *Tectonics*, *41*(6). https://doi.org/10.1029/2022tc007252
Montero-López, C., del Papa, C., Hongn, F., Strecker, M. R., & Aramayo, A. (2018). Synsedimentary broken-foreland tectonics during the Paleogene in the Andes of NW Argentine: New evidence from regional to centimetre-scale deformation features. *Basin Research*, *30*(S1), 142–159. https://doi.org/10.1111/bre.12212
Noetinger, S., & di Pasquo, M. (2013). New palynological information from the subsurface Copo, Caburé and Rincón formations (upper Lochkovian—Emsian), Salta Province, Argentina. *Memoir of the Association of Australasian Palaeontologists*, *44*, 107–121.
Payrola, P., Powell, J., del Papa, C., & Hongn, F. (2009). Middle Eocene deformation–sedimentation in the Luracatao Valley: Tracking the beginning of the foreland basin of northwestern Argentina. *Journal of South American Earth Sciences*, *28*(2), 142–154. https://doi.org/10.1016/j.jsames.2009.06.002
Prezzi, C. B., Götze, H.-J., & Schmidt, S. (2014). Andean foreland evolution and flexure in NW Argentina: Chaco–Paraná Basin. *Tectonophysics*, *628*, 228–243. https://doi.org/10.1016/j.tecto.2014.04.041
Sclater, J. G., & Christie, P. A. F. (1980). Continental stretching: An explanation of the Post-Mid-Cretaceous subsidence of the central North Sea Basin. *Journal of Geophysical Research*, *85*(B7), 3711–3739. https://doi.org/10.1029/JB085iB07p03711
Toth, J., Kusznir, N. J., & Flint, S. S. (1996). A flexural isostatic model of lithosphere shortening and foreland basin formation: Application to the Eastern Cordillera and Subandean belt of NW Argentina. *Tectonics*, *15*(1), 213–223. https://doi.org/10.1029/95TC02291
Zhou, R., Schoenbohm, L. M., Sobel, E. R., Davis, D. W., & Glodny, J. (2017). New constraints on orogenic models of the southern Central Andean Plateau: Cenozoic basin evolution and bedrock exhumation. *GSA Bulletin*, *129*(1–2), 152–170. https://doi.org/10.1130/b31384.1